



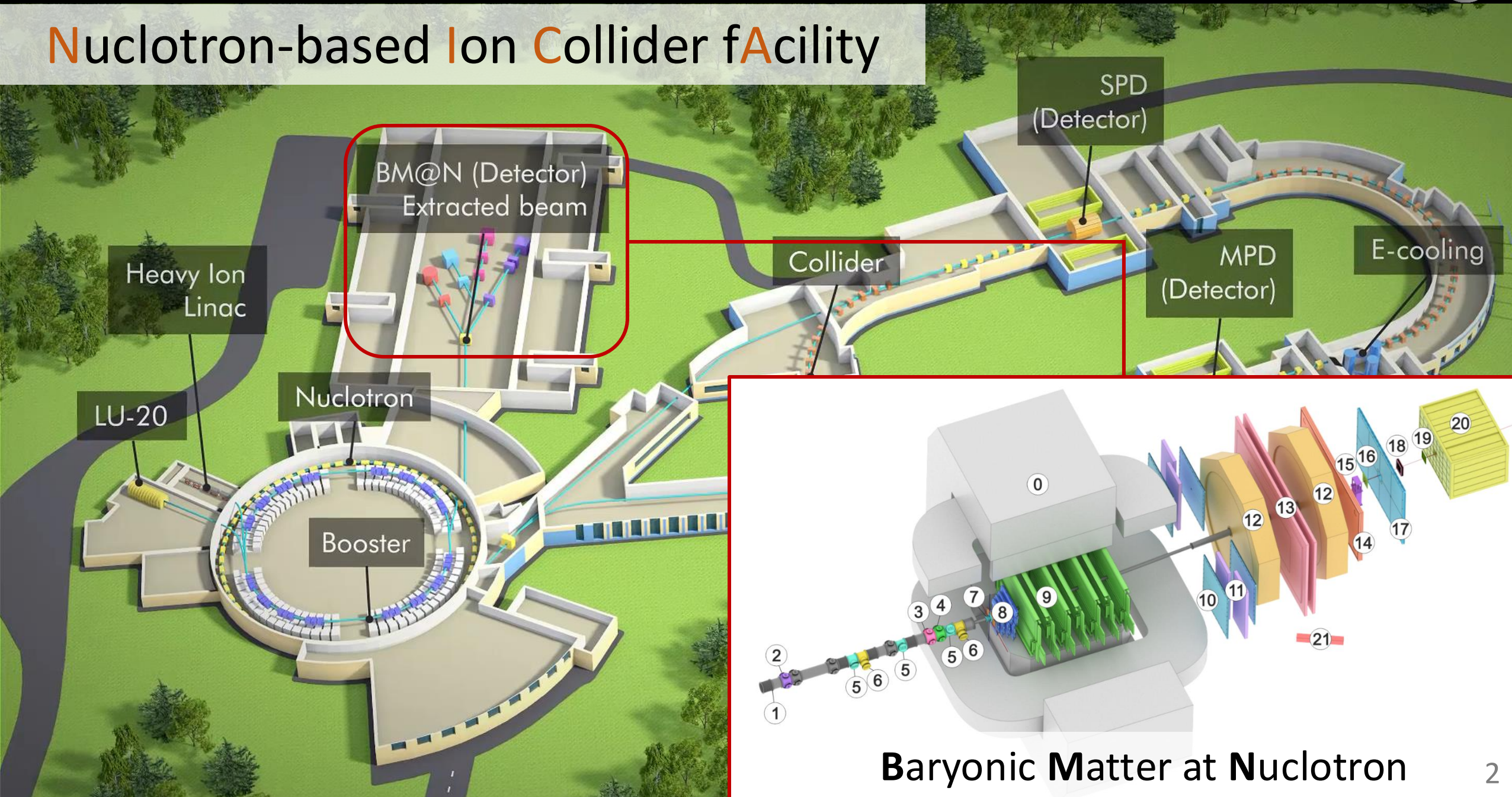
Measurement of neutron yields in the Xe+CsI reaction by the Highly Granular time-of-flight Neutron Detector prototype in the BM@N experiment

A. Zubankov on behalf of the HGND group

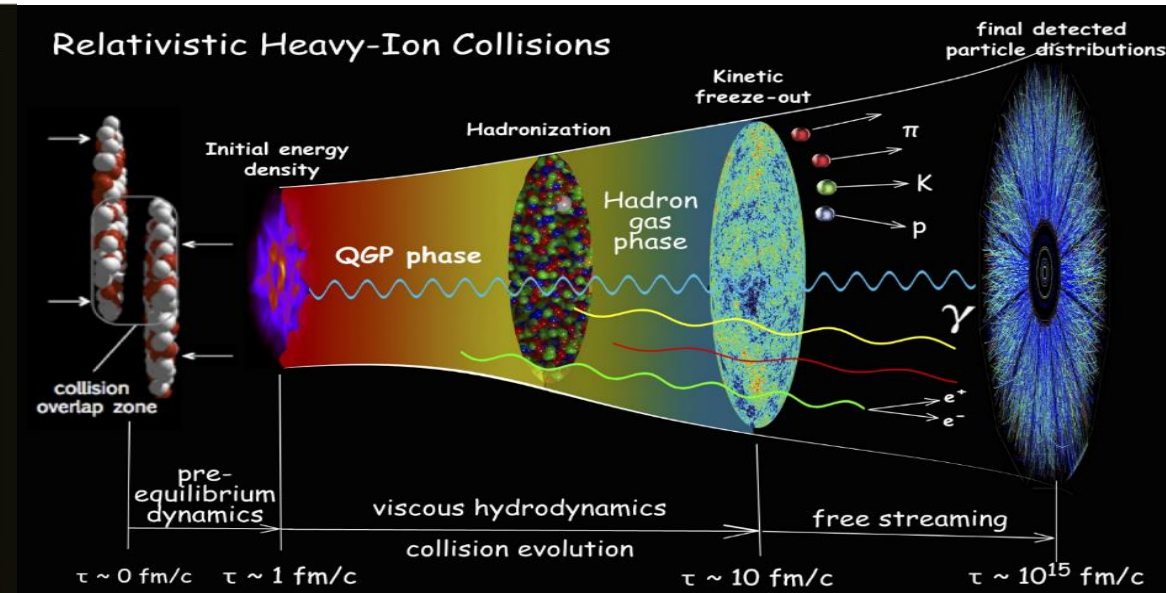
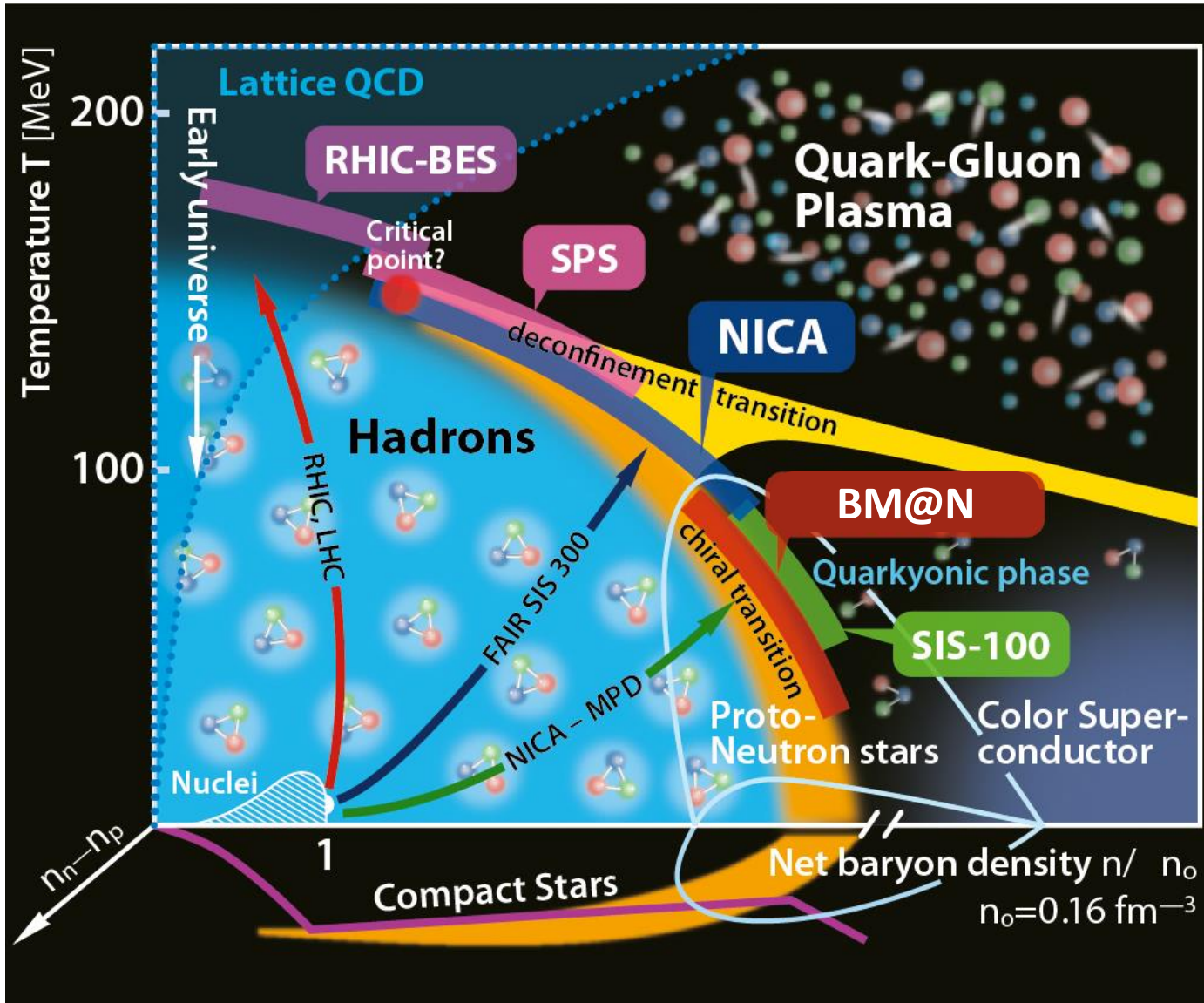
05.07.2025

BM@N is the first operational experiment at the NICA complex

Nuclotron-based Ion Collider facility



Baryonic Matter at Nuclotron



- Study of the QCD diagram at high baryon densities
- Study of the formation of multi-strange hyperons
- Search for hypernuclei in nucleus-nucleus collisions
- Study of the azimuthal asymmetry of charged particle yields in collisions of heavy nuclei.



- The Highly Granular Neutron Detector (HGND) at the BM@N experiment is under development for measuring the energy of neutrons up to 4 GeV produced in nucleus-nucleus collisions.
- Neutron measurements are necessary to obtain robust information on the symmetry energy of the Equation of State for high baryon density matter.
- A compact HGND prototype has already been designed and constructed to validate the concept of the full-scale HGND.
- For the first time, small prototype of the HGND was used in $^{124}\text{Xe}+\text{CsI}$ at 3.8A GeV run at the BM@N.
- The neutron yields in the HGND prototype and cross sections were evaluated with model-estimated efficiencies for central and semi-central collisions and for electromagnetic dissociation (EMD) of ^{124}Xe .

1. Design of **H**ighly **G**ranular **N**eutron **D**etector prototype
2. Event selection and neutron reconstruction
3. HGND prototype efficiencies and acceptances estimations
 - 3.1. EMD modeling with RELDIS
 - 3.2. Hadronic interactions modeling with DCM-QGSM-SMM and UrQMD-AMC (in Cascade mode)
4. Neutron yields and cross sections estimation

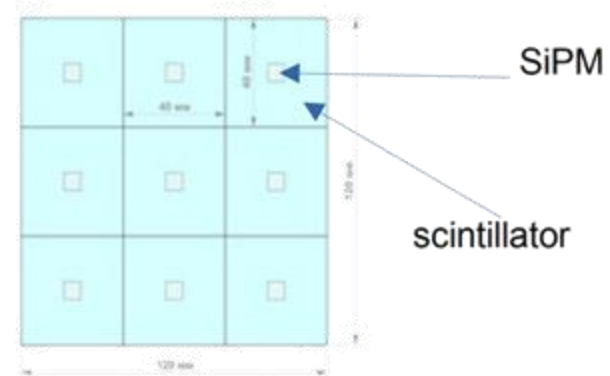
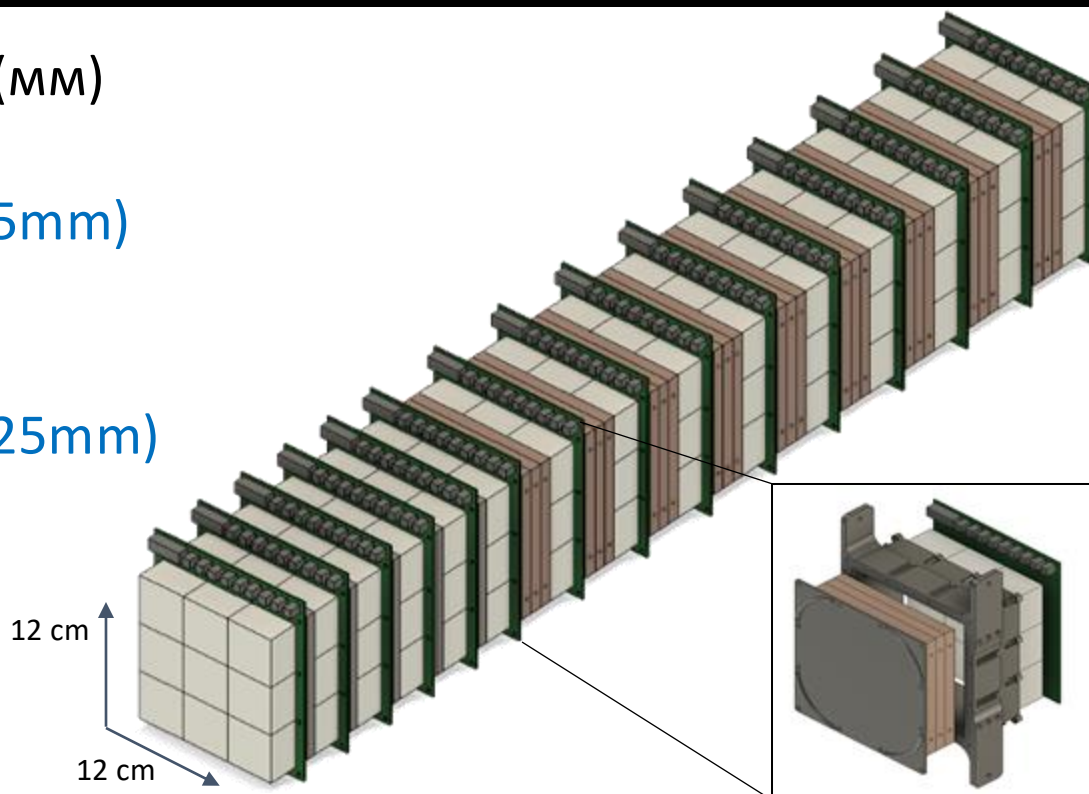
1. Design of **Highly Granular Neutron** **Detector prototype**

HGND prototype design



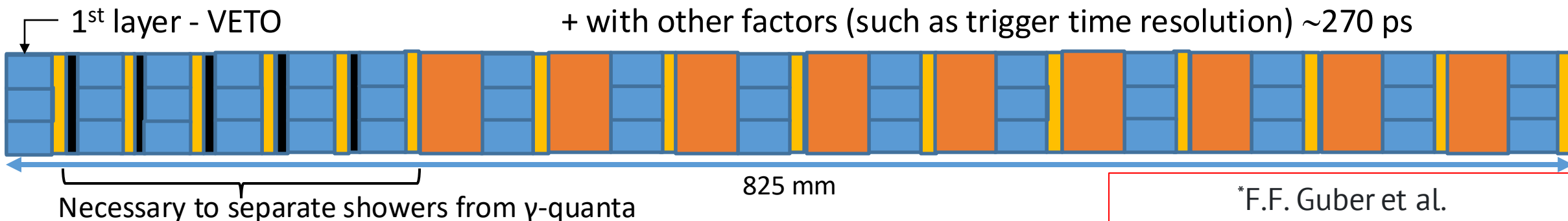
- Scint. layer **Veto** 120x120x25 (mm)
- 1st (electromagnetic) part:
5 layers: Pb (8mm) + Scint. (25mm)
+ PCB + air
- 2nd (hadronic) part:
9 layers: Cu (30mm) + Scint. (25mm)
+ PCB + air

Scint. cell – 40 x 40 x 25 mm³
 Total number of cells – 135
 Total size – 12 x 12 x 82.5 cm³
 Total length ~ 2.5 λ_{int}



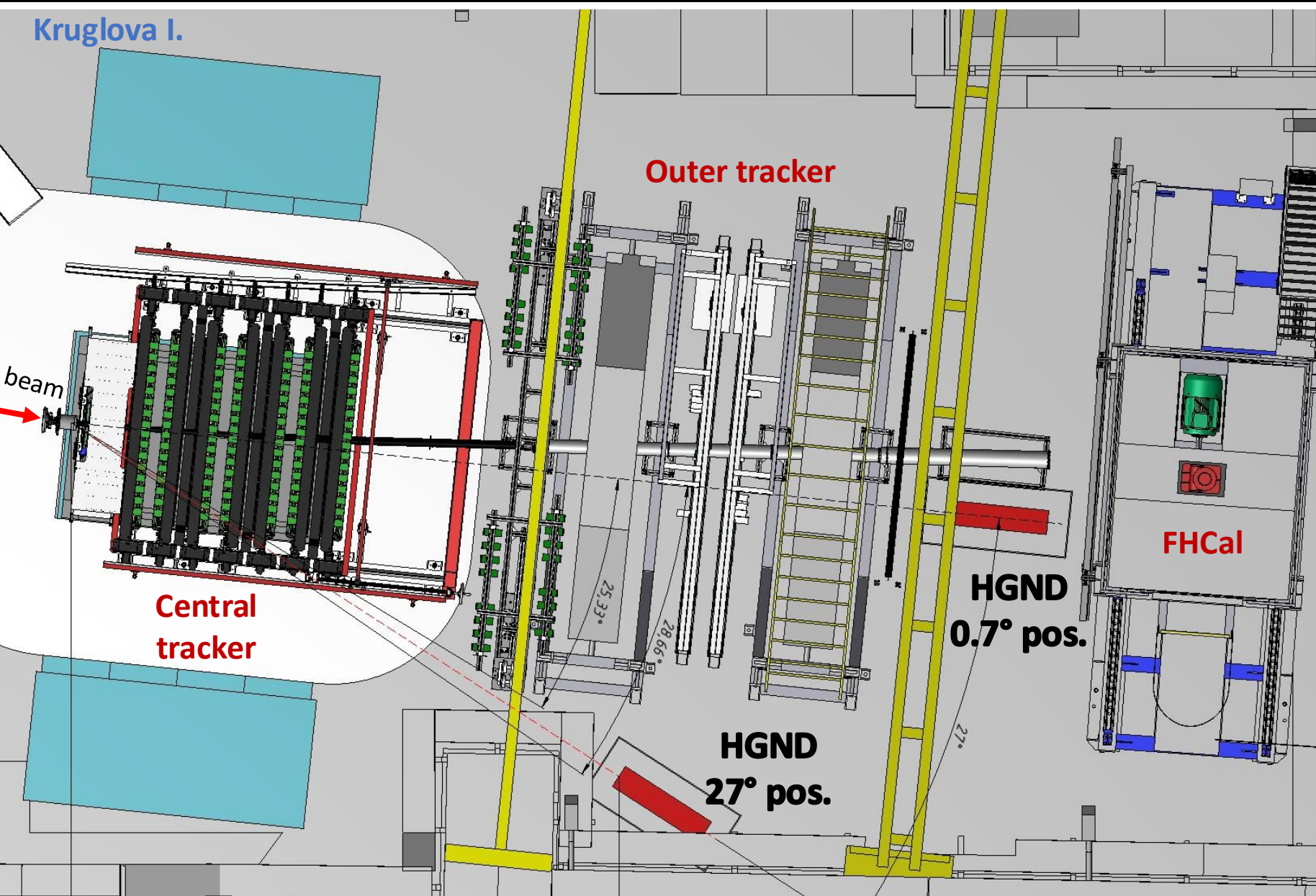
Hamamatsu S13360- 6050PE
 Photosensitive area – 6x6 mm²
 Number of pixels – 14400
 Pixel size – 50 μm
 Gain – 1.7×10^6
 PDE – 40%

Time resolution of cell ~200 ps*,
 + with light collection heterogeneity ~240 ps,
 + with other factors (such as trigger time resolution) ~270 ps



*F.F. Guber et al.
 10.1134/S0020441223030065

HGND prototype in the Xe+CsI@3.8A GeV run of BM@N



27° position:

Measurements of the neutron spectrum at \sim midrapidity.

0° position:

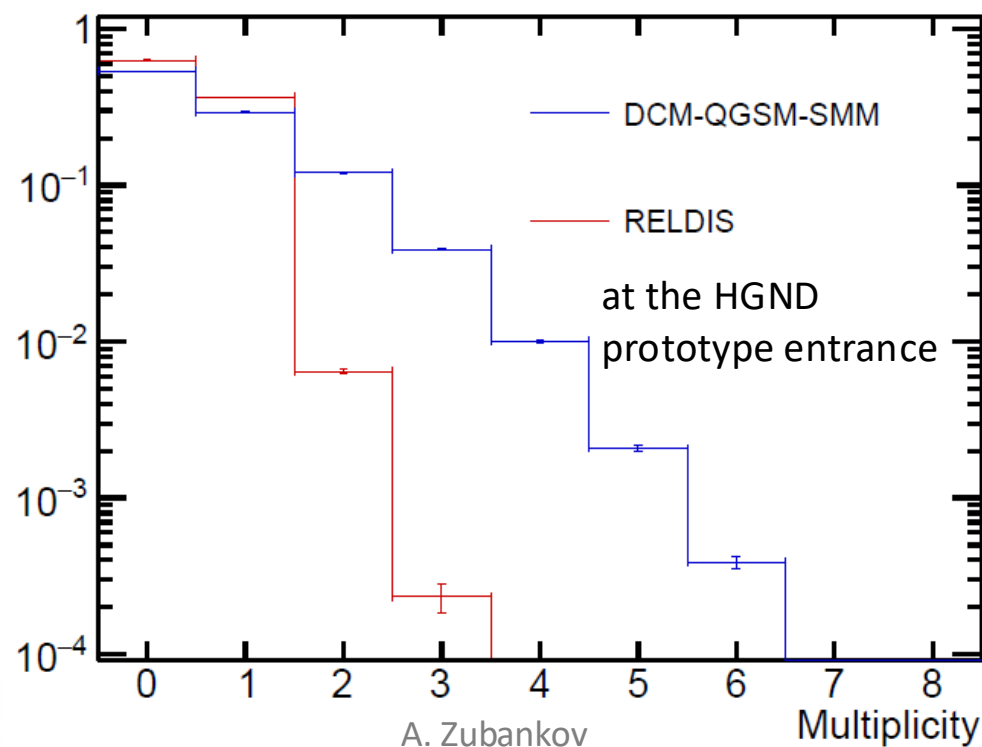
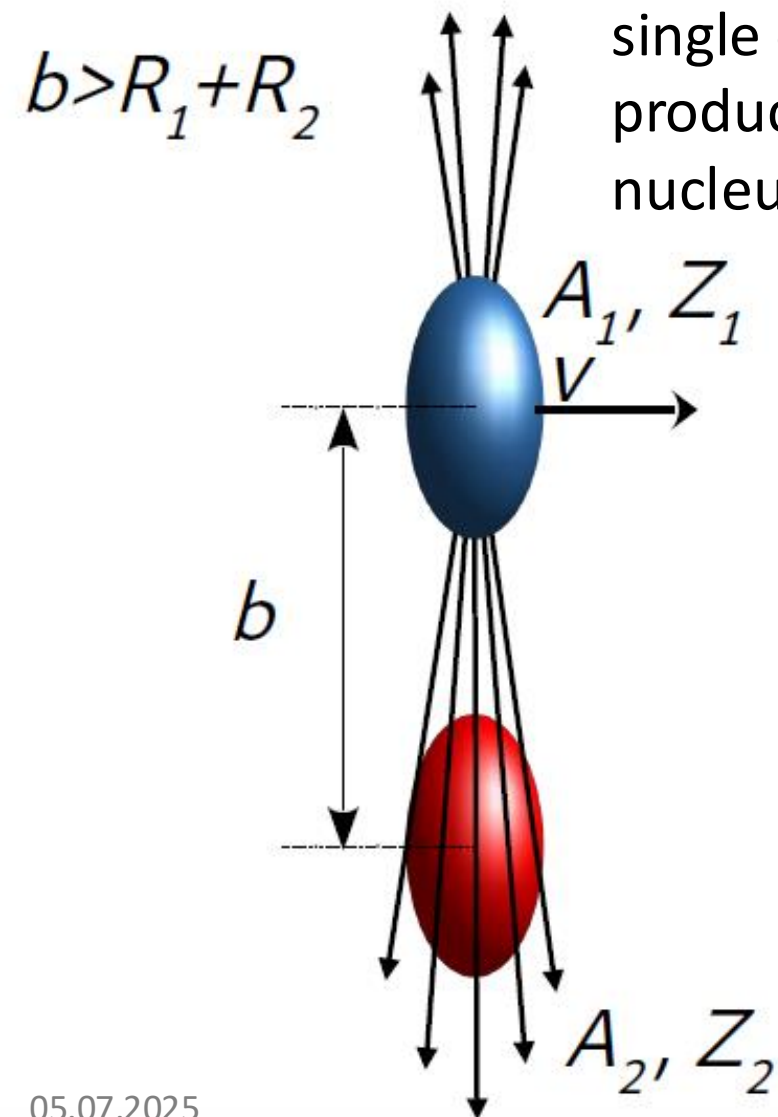
Test and calibration with known neutron energy (energy of a beam of spectator neutrons)



2. Event selection and neutron reconstruction

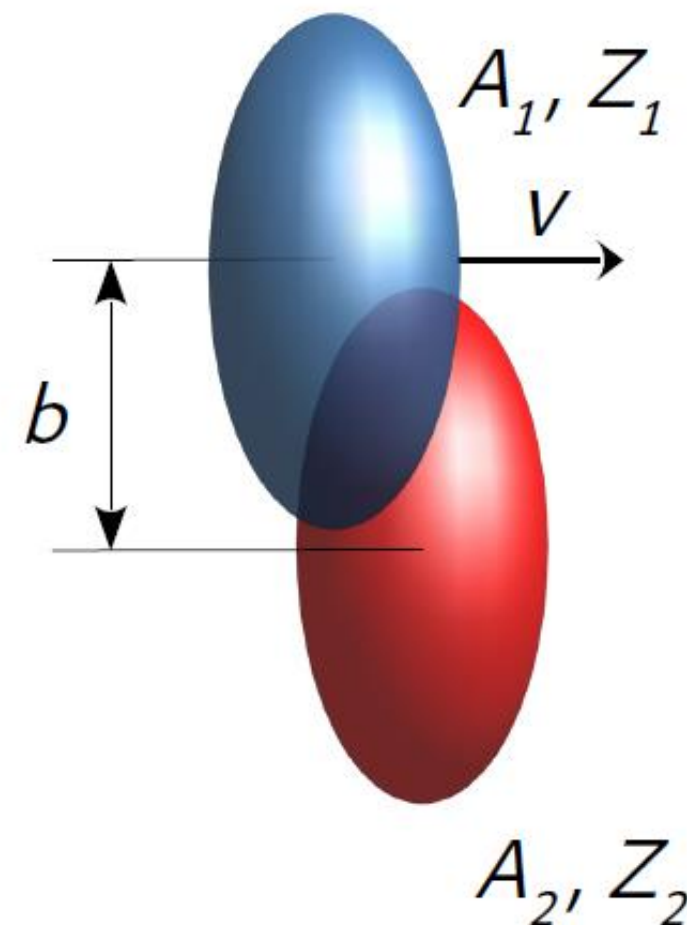
EMD:

In most cases, EMD of a heavy nucleus results in the emission of a single or just few neutrons with the production of a single residual nucleus



Hadronic interactions:

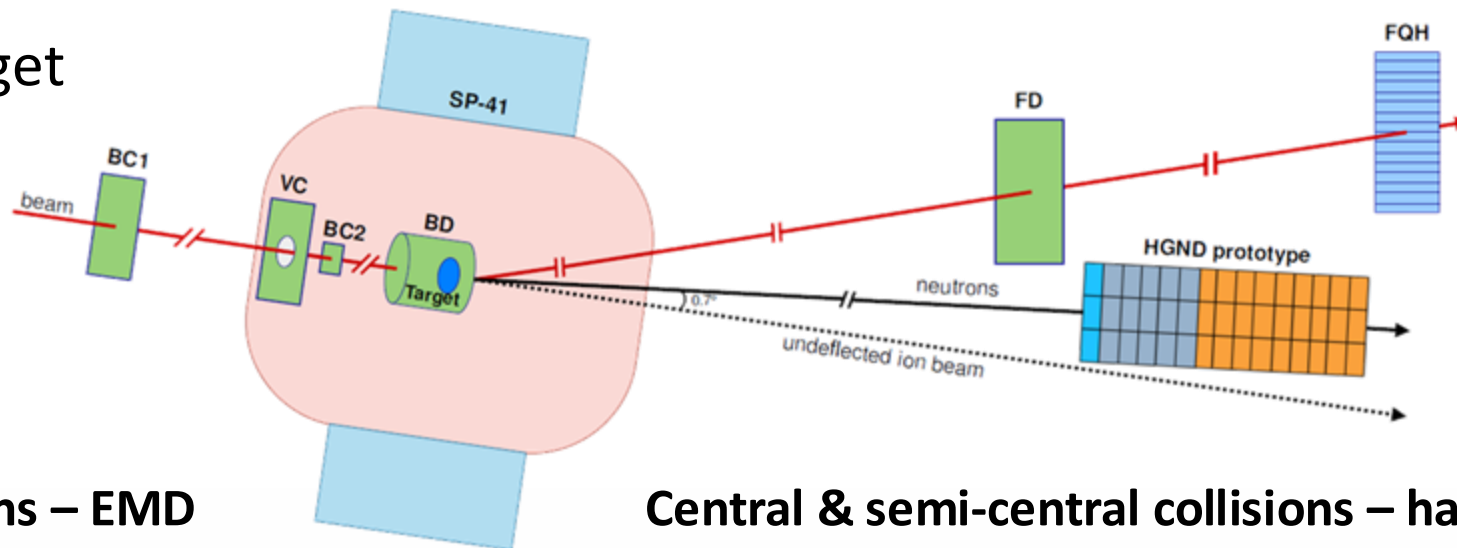
$$b < R_1 + R_2$$



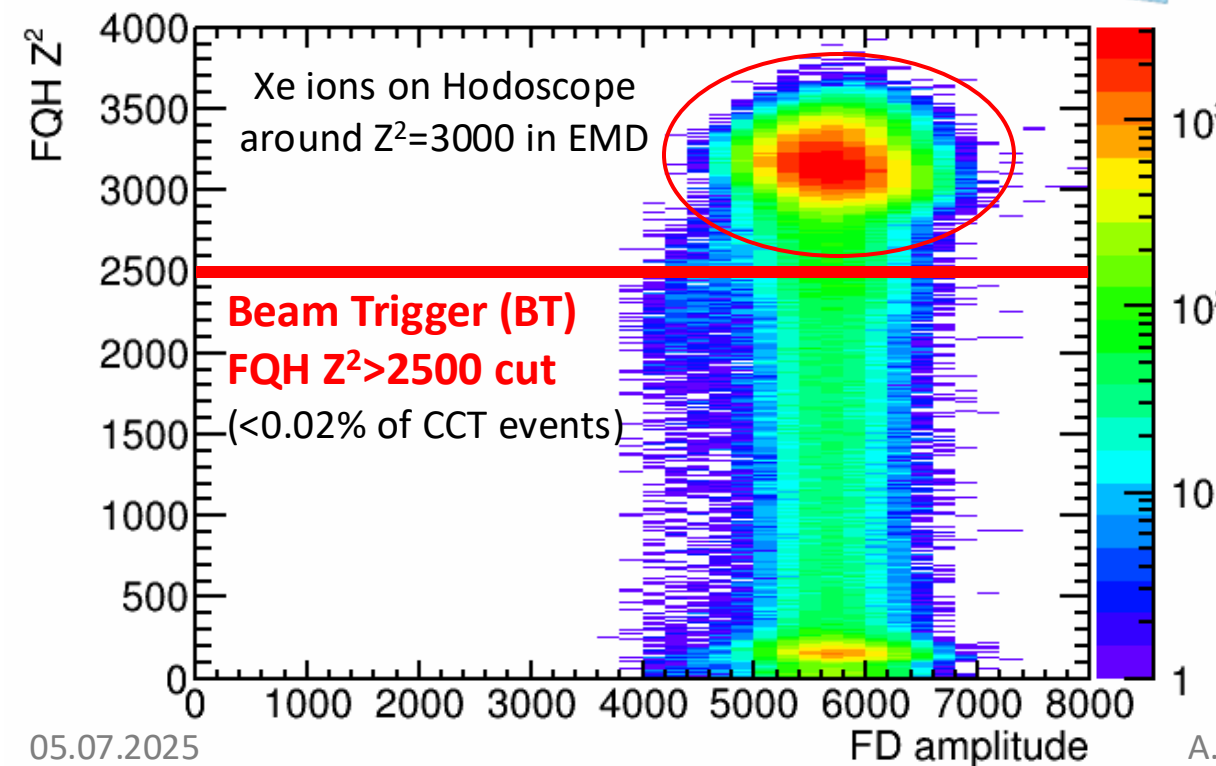
Event selection for EMD and hadronic interactions



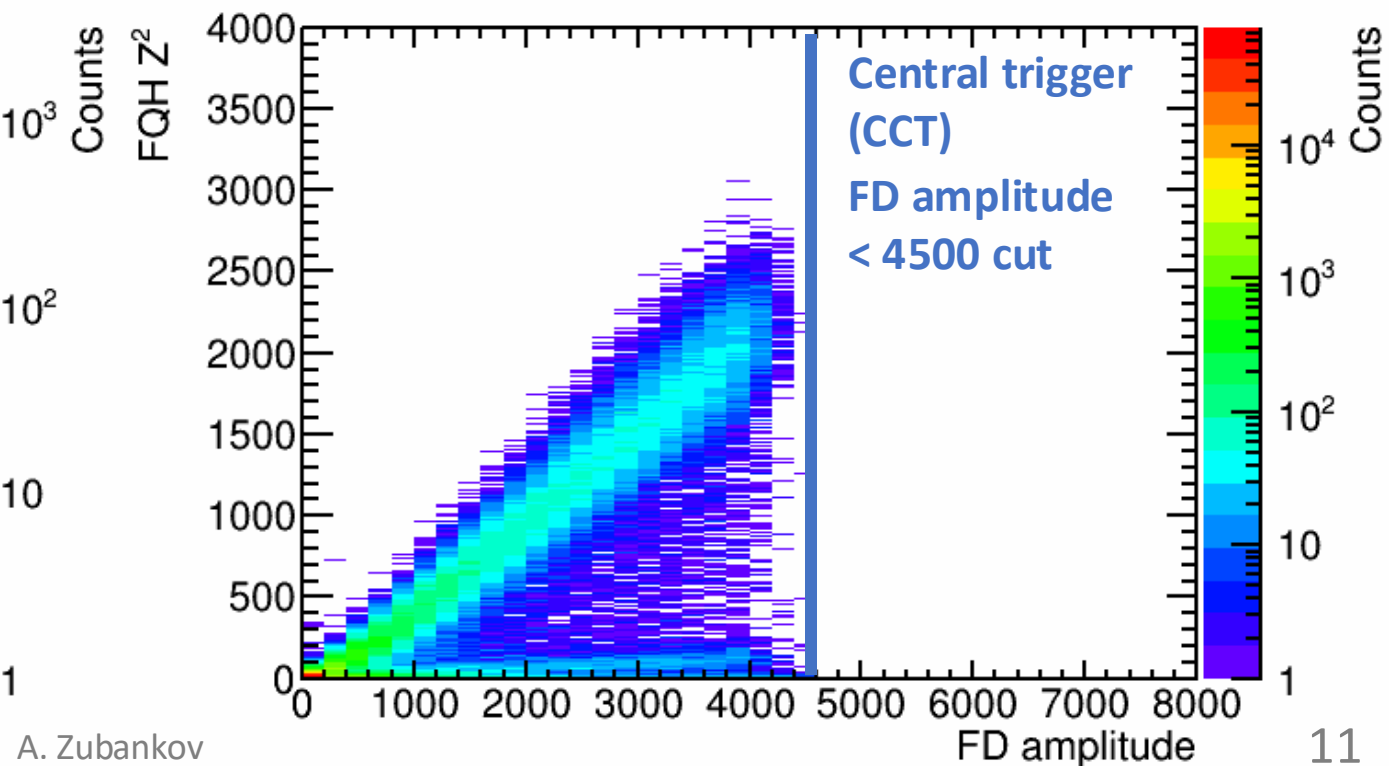
Only single Xe ion in target



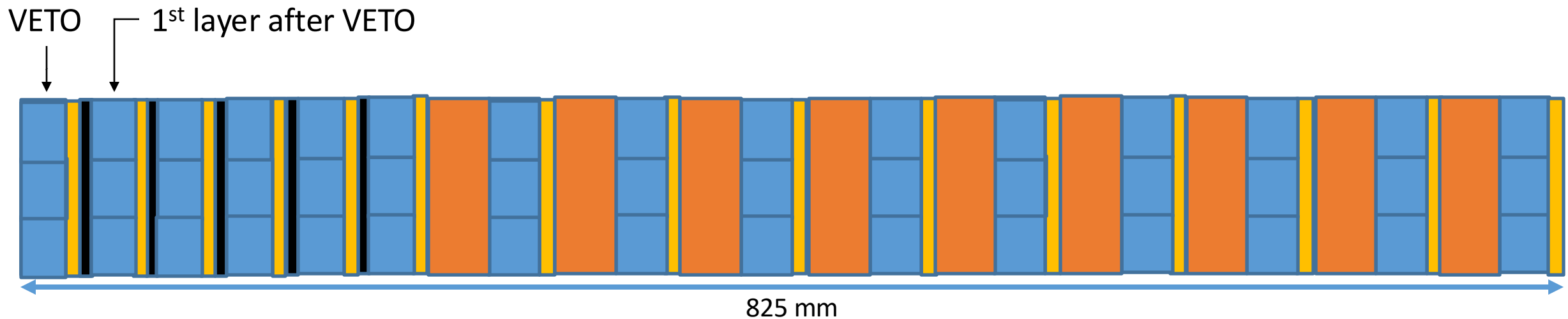
Ultra-peripheral collisions – EMD

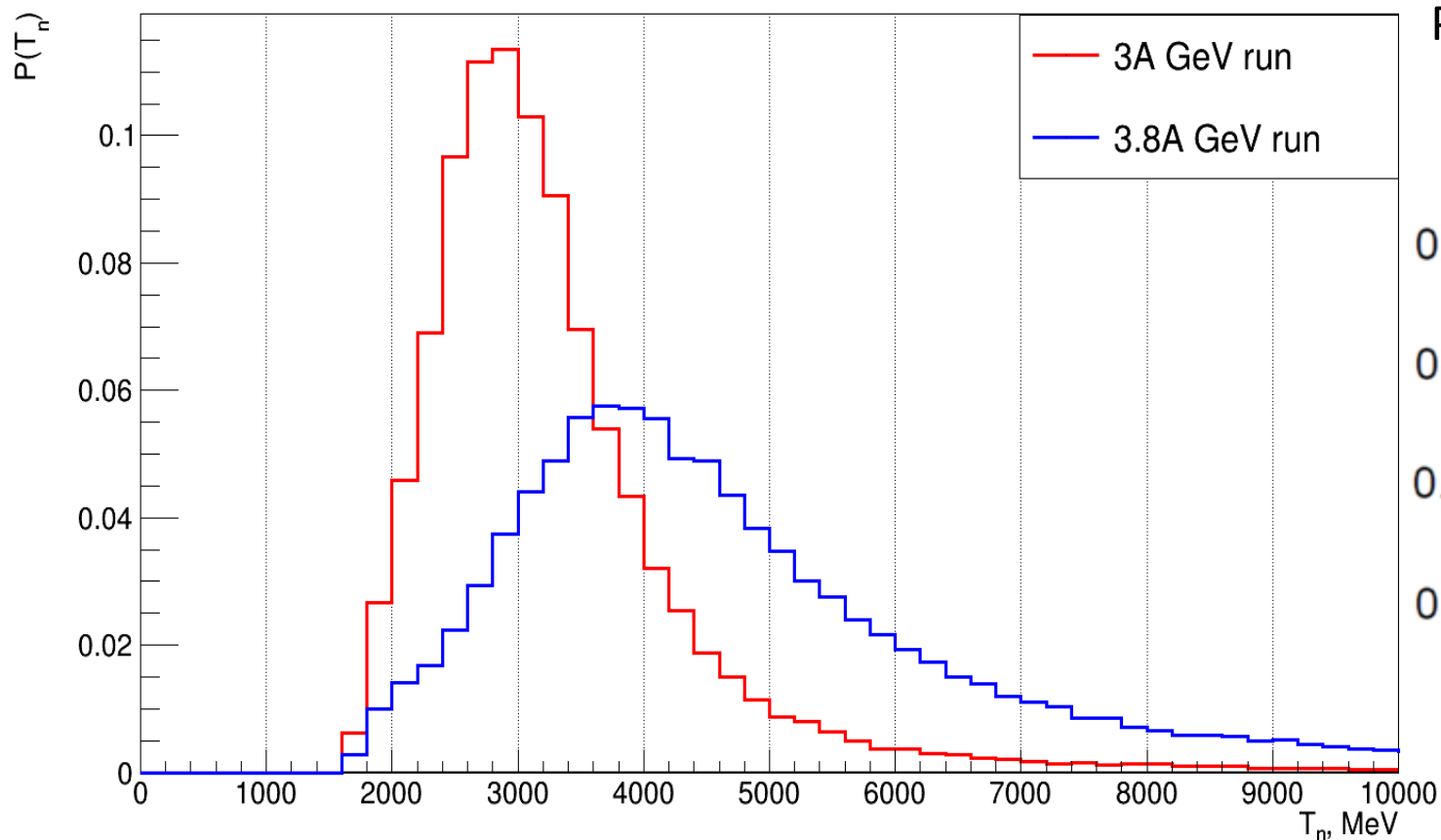


Central & semi-central collisions – hadronic interactions

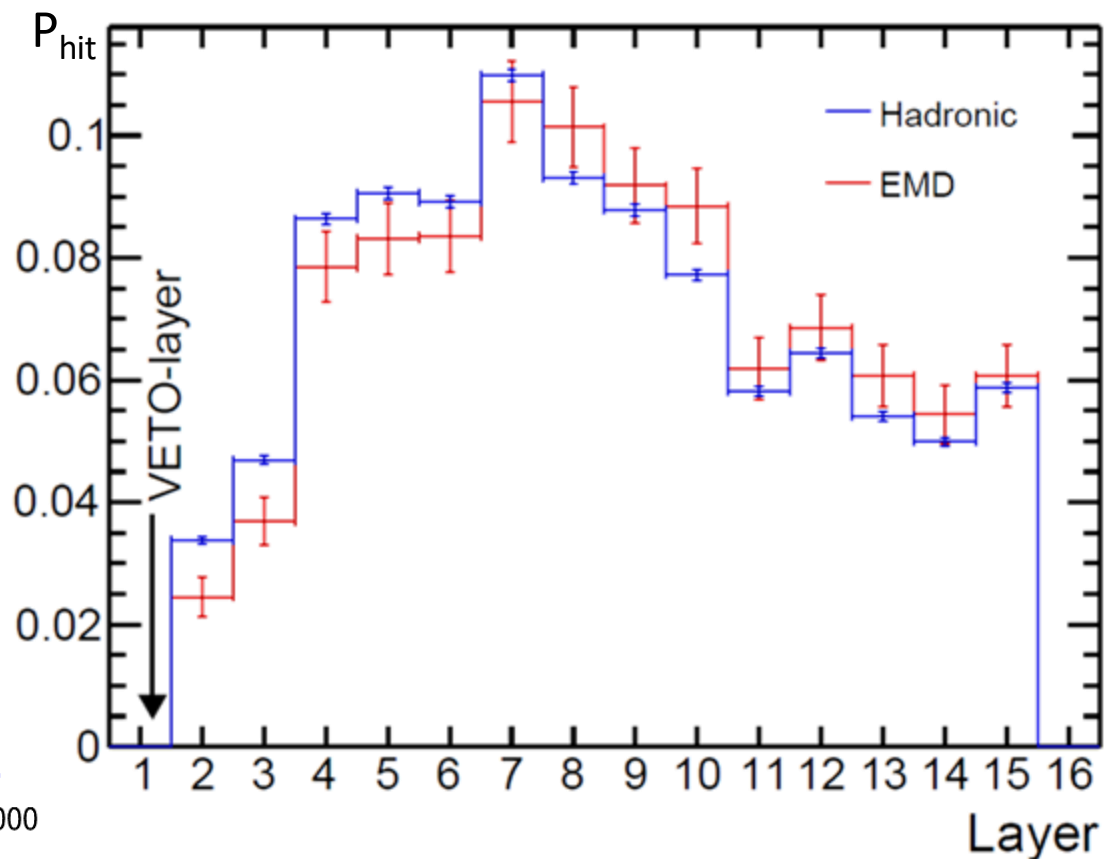


- Selection of events without charged particles using **VETO**
- Background rejection from spectator neutrons using **ToF cut**
- Photon rejection using **1st layer after VETO** ($1.55 X_0$ or $0.11 \lambda_{\text{int}}$)
- Reconstruction of energy by **maximum velocity**
- Scaled by incident ion beam rate measured by **Beam Trigger BT**



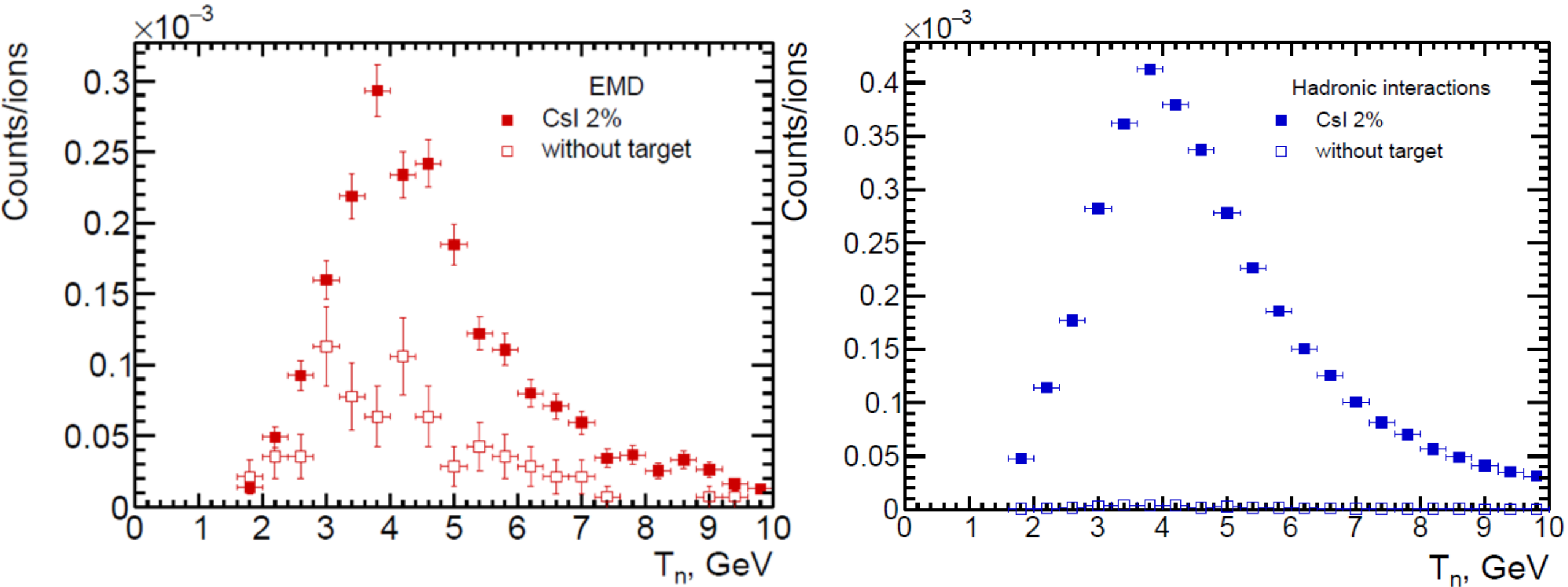


Reconstructed neutron spectra for both 3A GeV and 3.8A GeV runs are in correct positions.



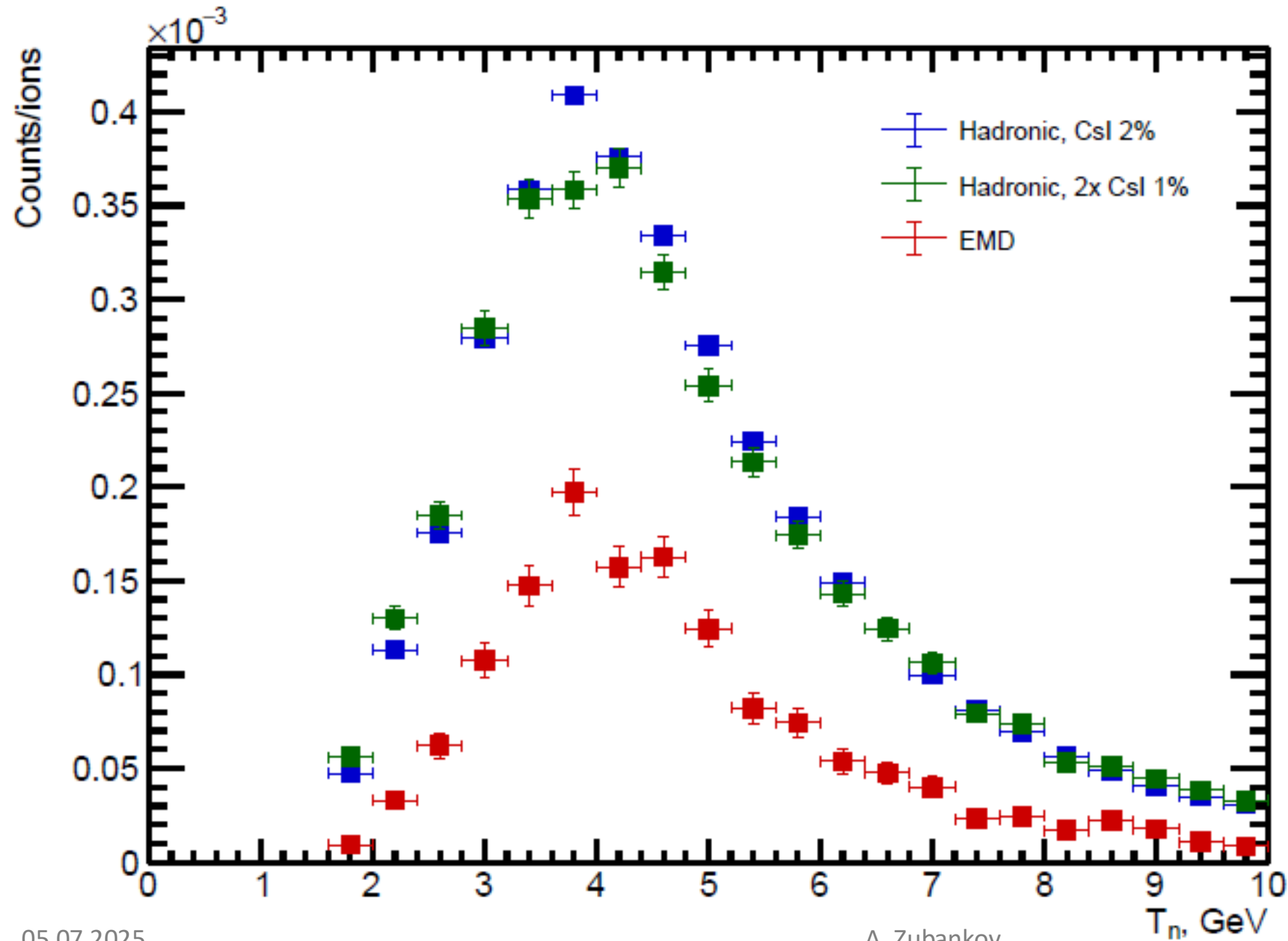
The highest first interaction probability for spectator neutron is at the beginning of the hadronic part (7th layer), as expected.

Reconstructed spectra for EMD and hadronic interactions



Reconstructed spectra was obtained for runs with Csl 2% target and without target to estimate part of non-target interactions.

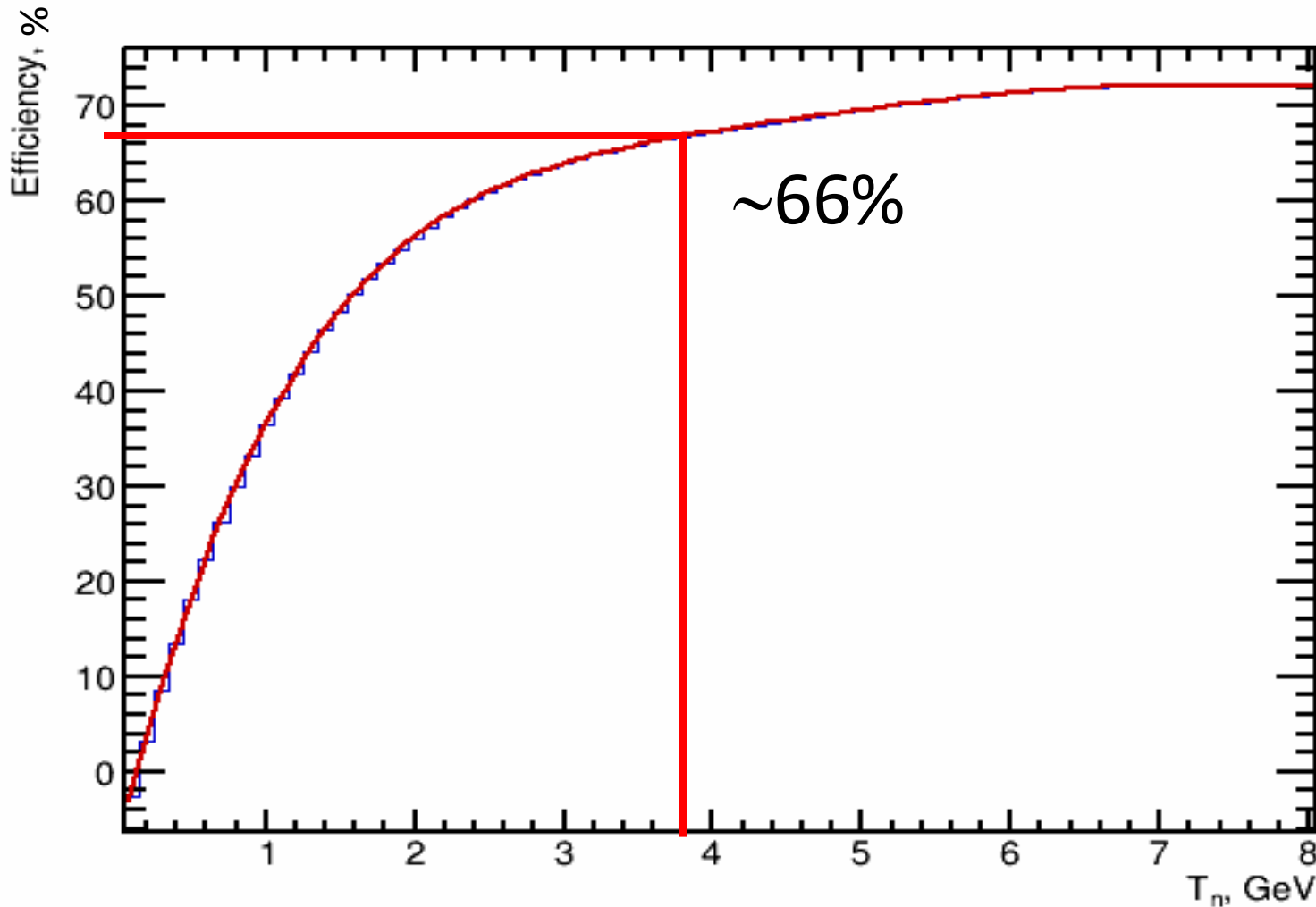
Then, empty target events were subtracted from target spectra.



Reconstructed spectra
after subtracting events
from empty target

Spectra with 1% and 2%
target are in good
agreement

3. HGND prototype efficiencies and acceptances estimations



Geant4 simulation:

Box generator, only neutrons

- VETO-cut
- γ -cut
- ToF cut

Then, we use the DCM-QGSM-SMM¹ and UrQMD-AMC² (in Cascade mode) models to estimate the detector efficiency for hadronic interactions, and RELDIS³ for EMD.

¹M. Baznat et al., Monte-Carlo Generator of Heavy Ion Collisions DCM-SMM, *Phys. Part. Nucl. Lett.* **2020**, 17, 303.

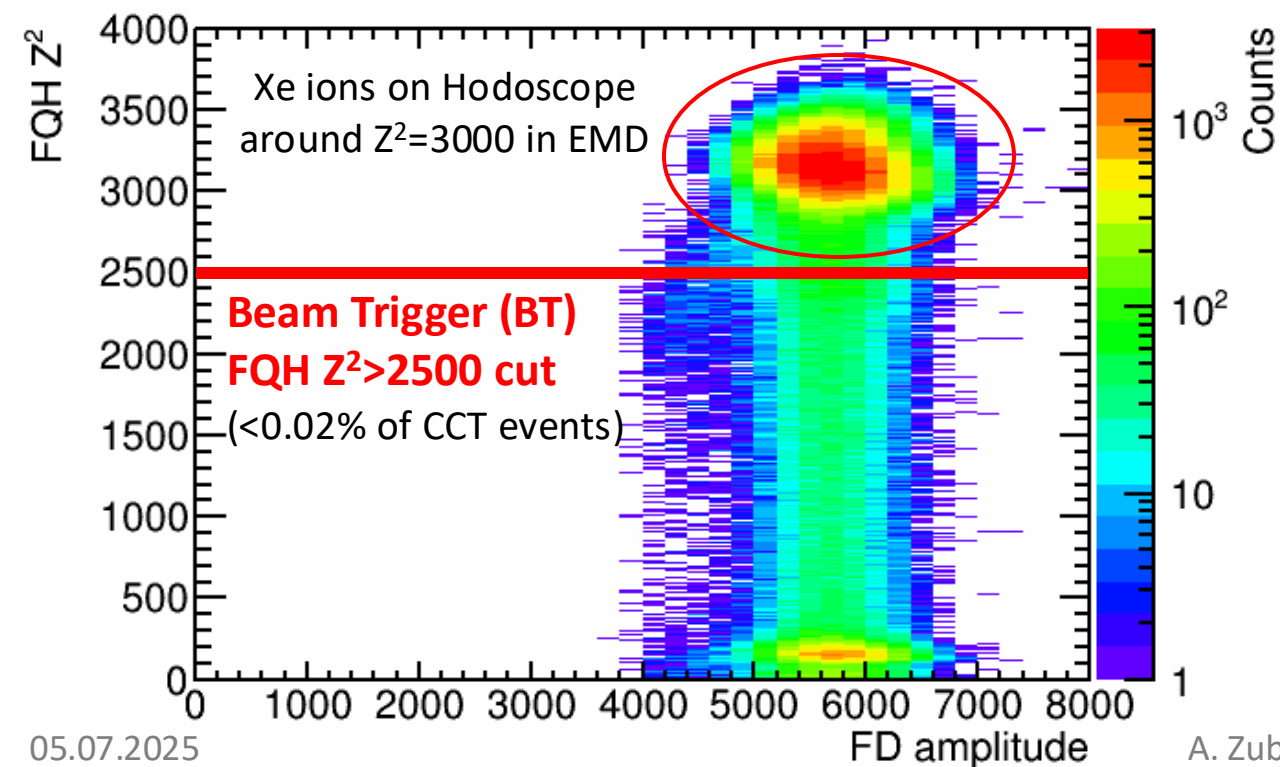
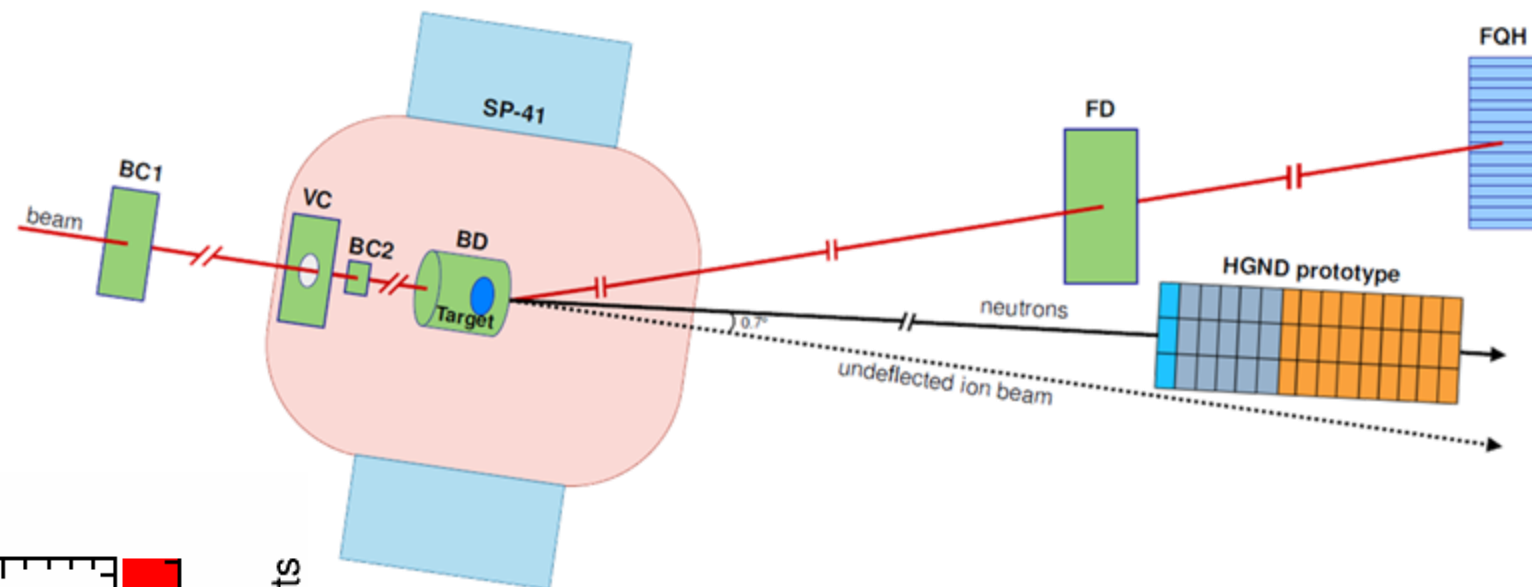
²See A. Svetlichnyi report – Production of spectator neutrons, protons and light fragments on fixed targets at NICA

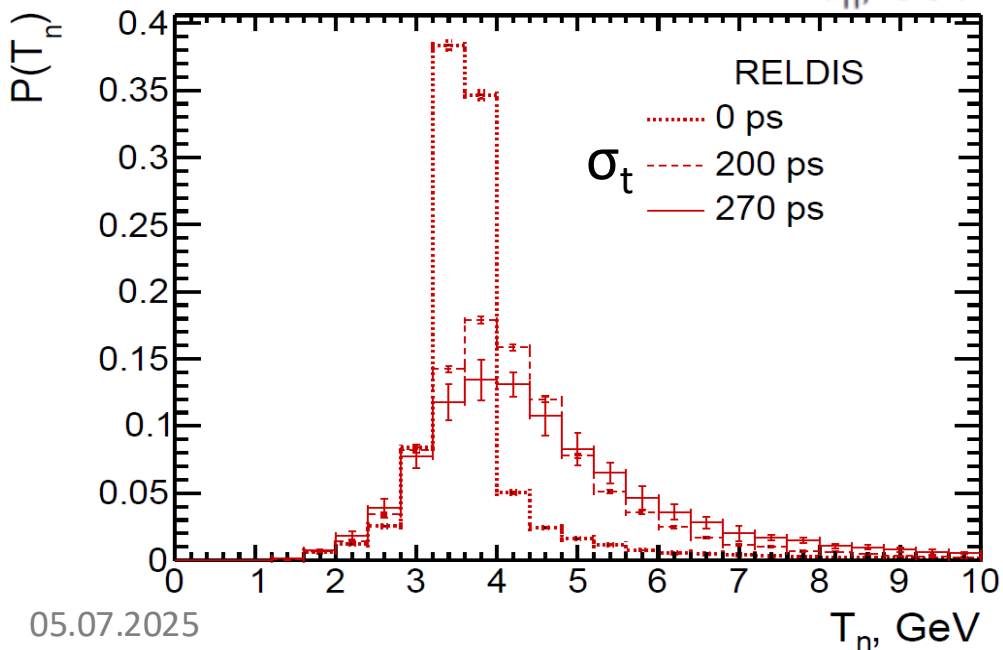
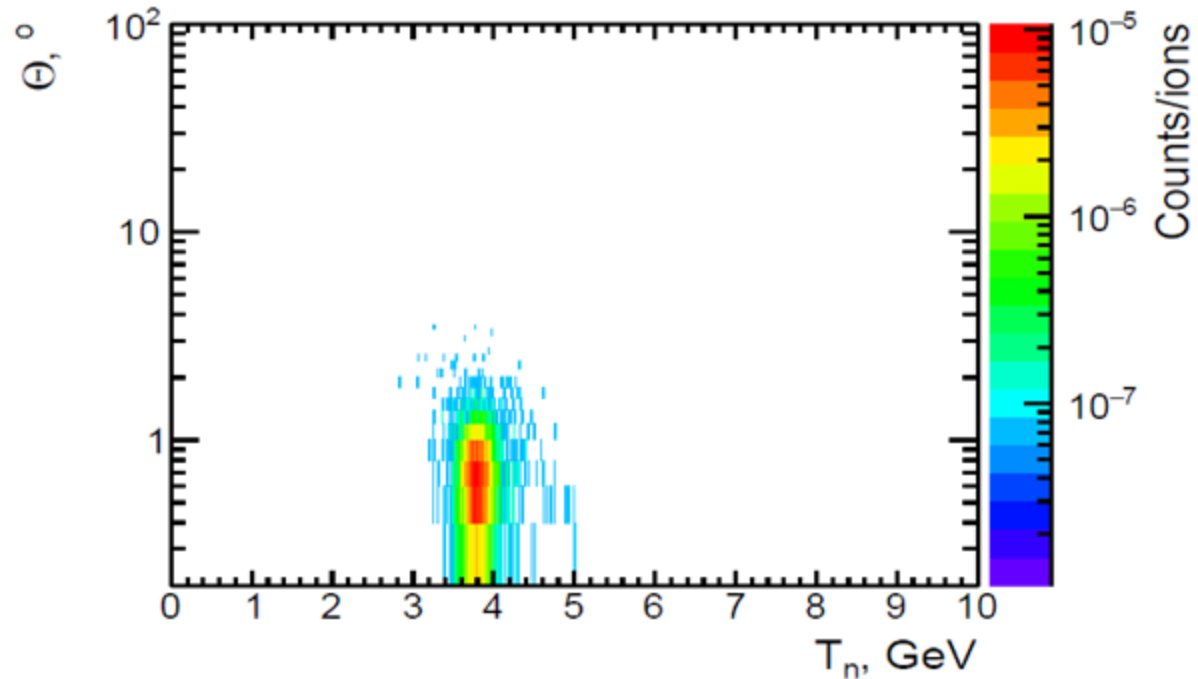
³I. Pshenichnov, Electromagnetic Excitation and Fragmentation of Ultrarelativistic Nuclei. *Phys. Part. Nucl.* **2011**, 42 (2), 215-250.

3.1. EMD modeling with RELDIS

Only single Xe ion in target

Ultra-peripheral collisions – EMD

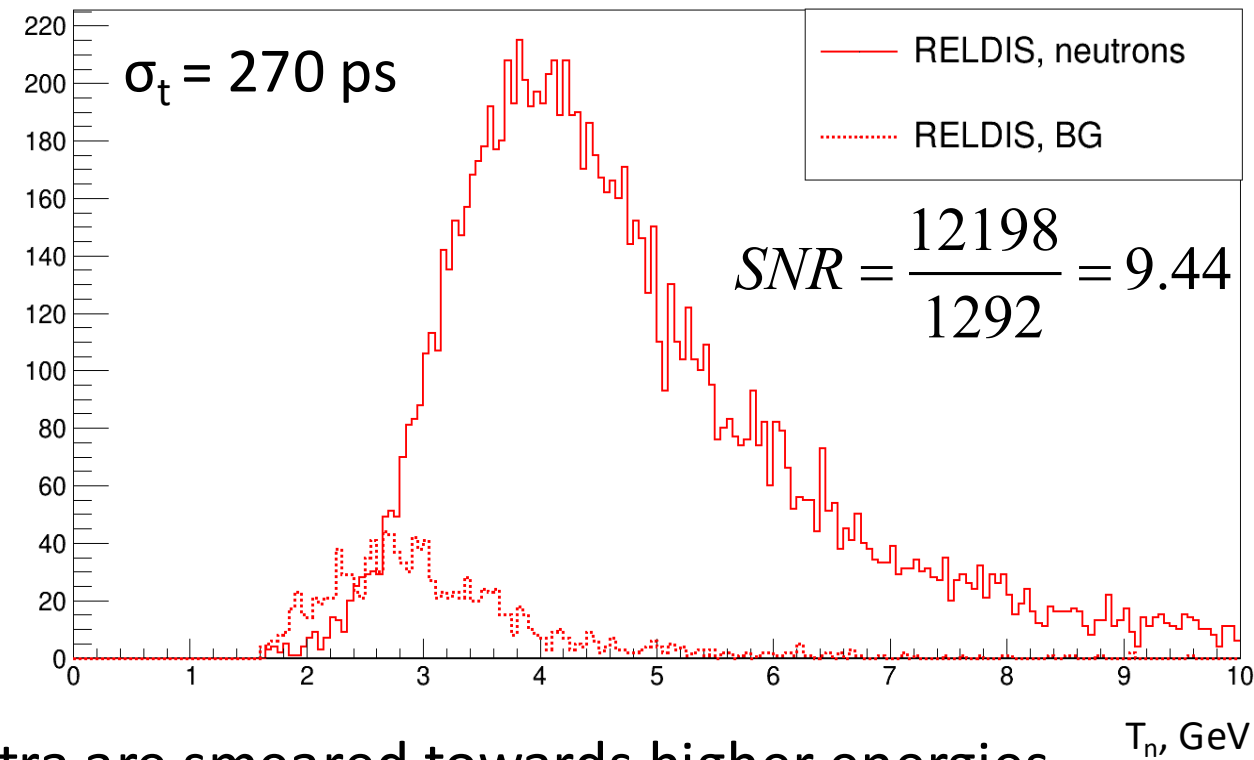




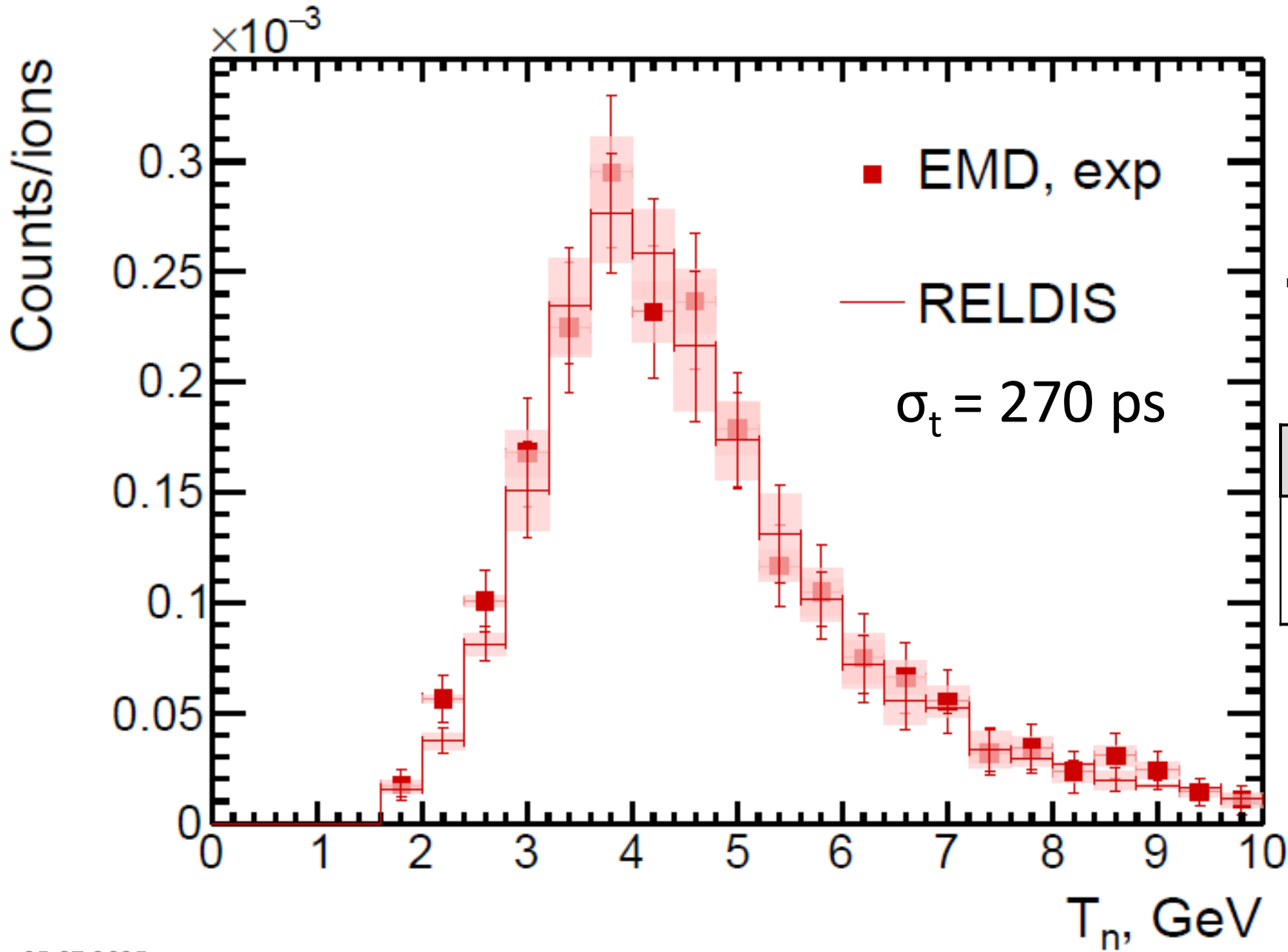
RELDIS model $^{124}\text{Xe} + ^{130}\text{Xe} @ 3.8\text{A GeV}$

Neutron multiplicity – **1.05**

Neutron multiplicity hitting the HGND prototype surface – **1.02**



The spectra are smeared towards higher energies due to the time resolution of about 270 ps.

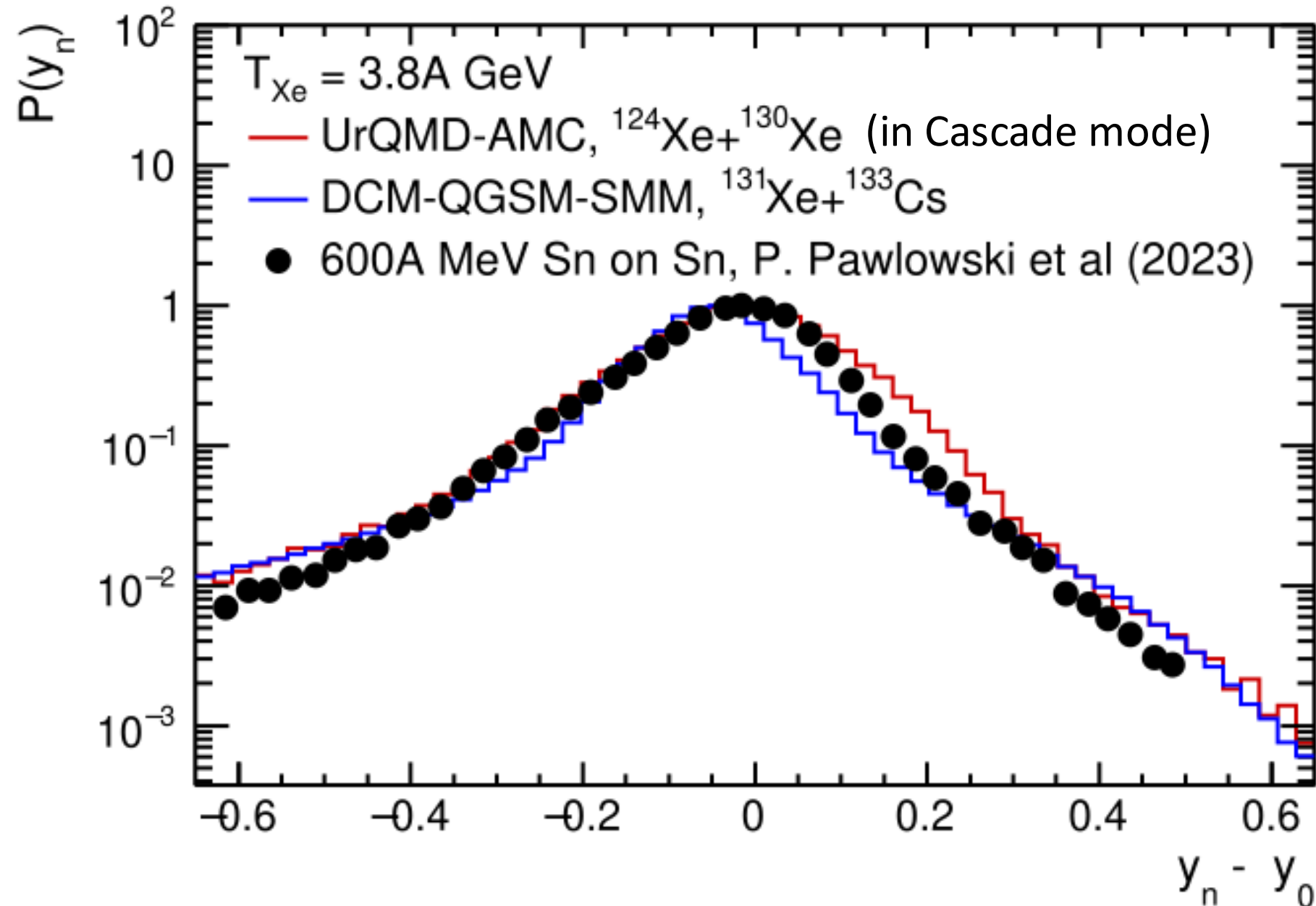


$$\Omega_n = \frac{N_{hit}}{N_{gen}} \quad \epsilon_n = \frac{N_{rec}}{N_{hit}}$$

Ω_n , %	ϵ_n , %	$\Omega_n \times \epsilon_n$, %
34.21 ± 0.25	60.06 ± 0.44	20.55 ± 0.15

The RELDIS model is in good agreement with the experimental data obtained.

3.2. Hadronic interactions modeling with DCM-QGSM-SMM and UrQMD-AMC (in Cascade mode)

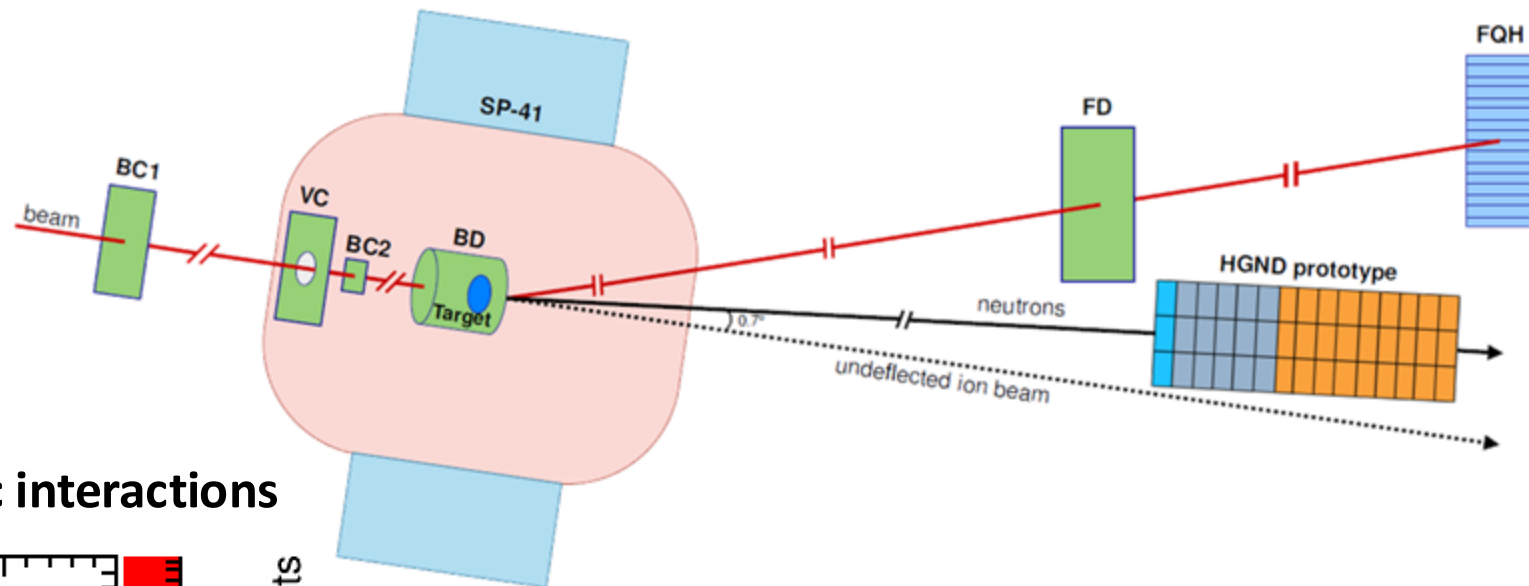


DCM-QGSM-SMM and UrQMD-AMC describe the experiment well in the rapidity region $y_n - y_0 < 0$.

In the region $y_n - y_0 > 0$, DCM-QGSM-SMM underestimates the data whereas UrQMD-AMC overestimates.

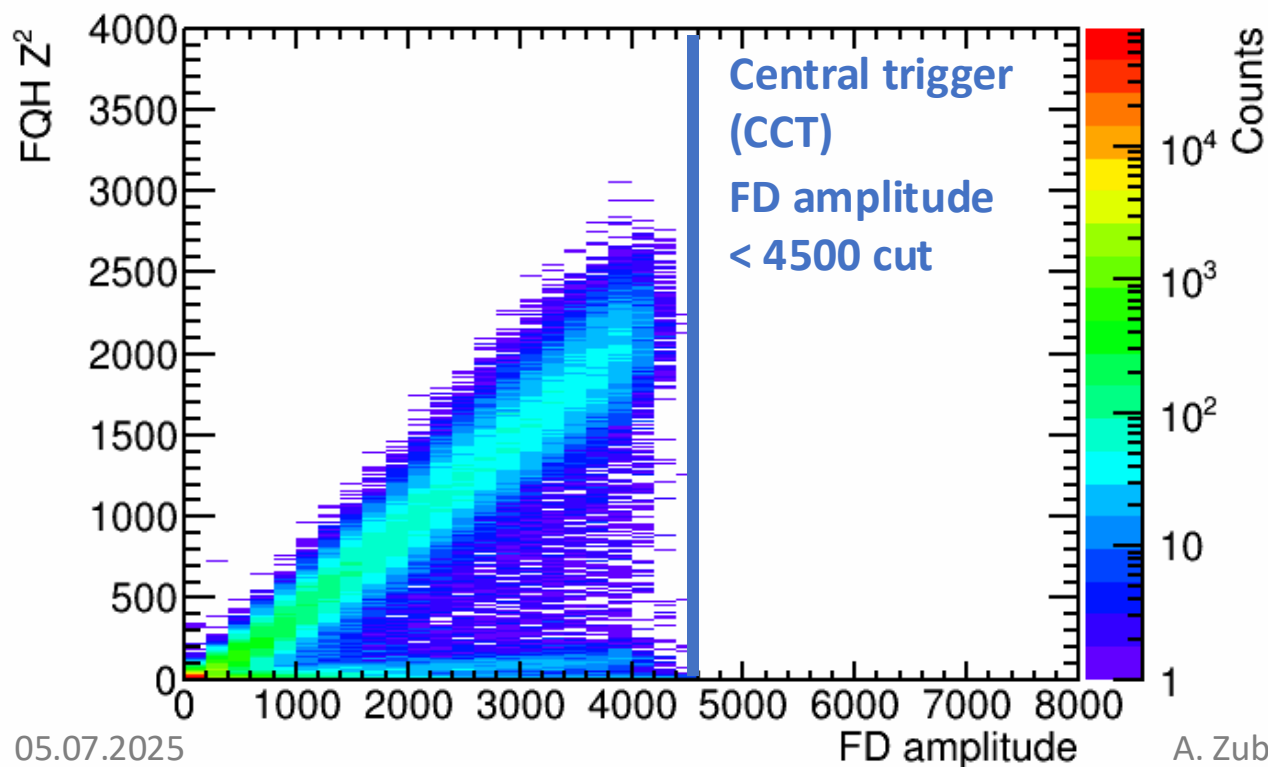
For DCM-QGSM-SMM, there is a shift in the rapidity relative to the beam rapidity.

Event selection for hadronic interactions in experiment



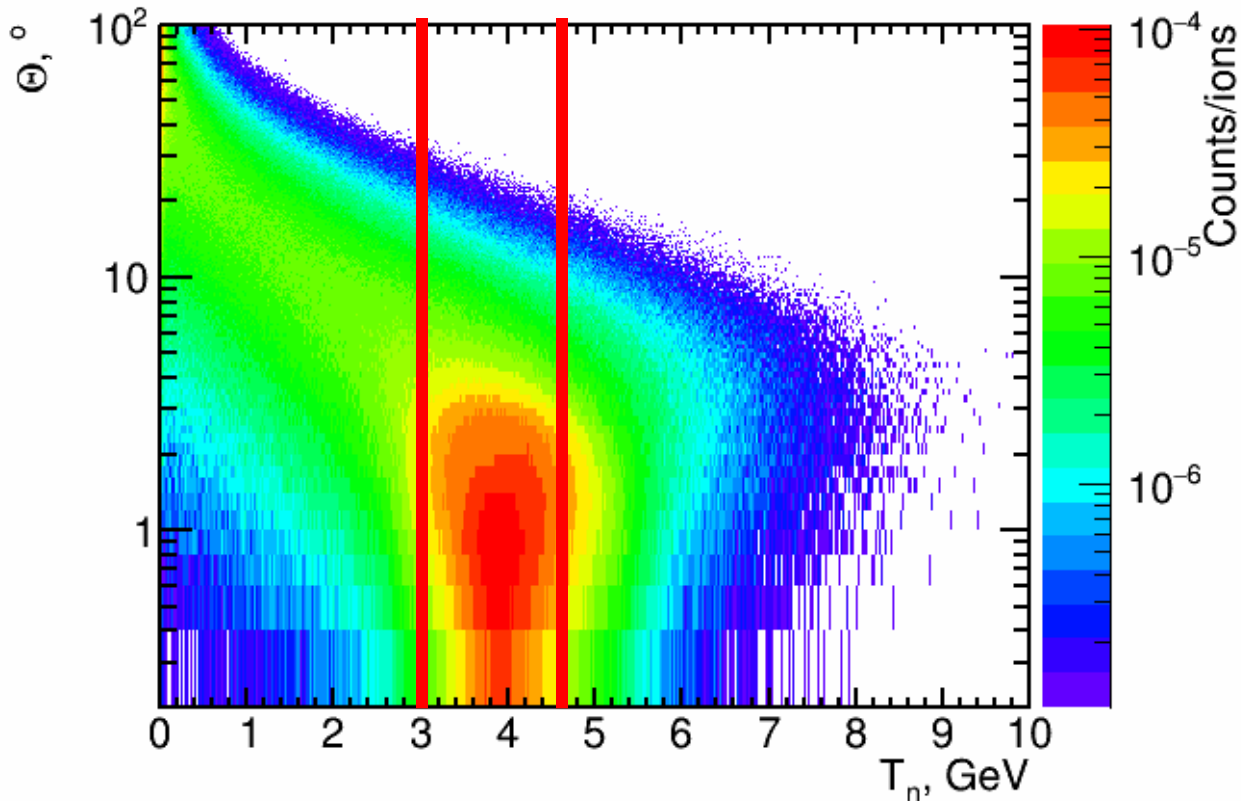
Only single Xe ion in target

Central & semi-central collisions – hadronic interactions



UrQMD-AMC (in Cascade mode)

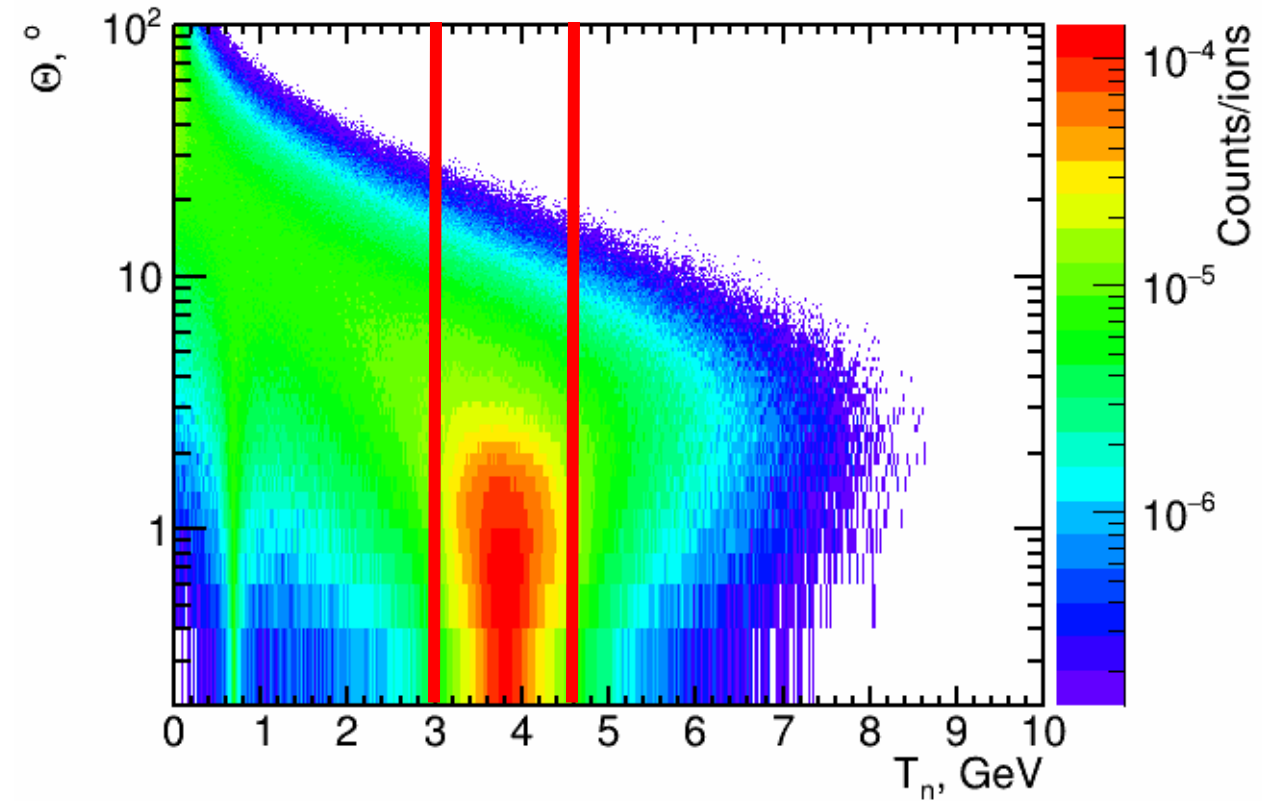
3.8A GeV $^{124}\text{Xe} + ^{130}\text{Xe}$



Spectator neutron multiplicity – **17.70**

DCM-QGSM-SMM

3.8A GeV $^{131}\text{Xe} + ^{133}\text{Cs}$

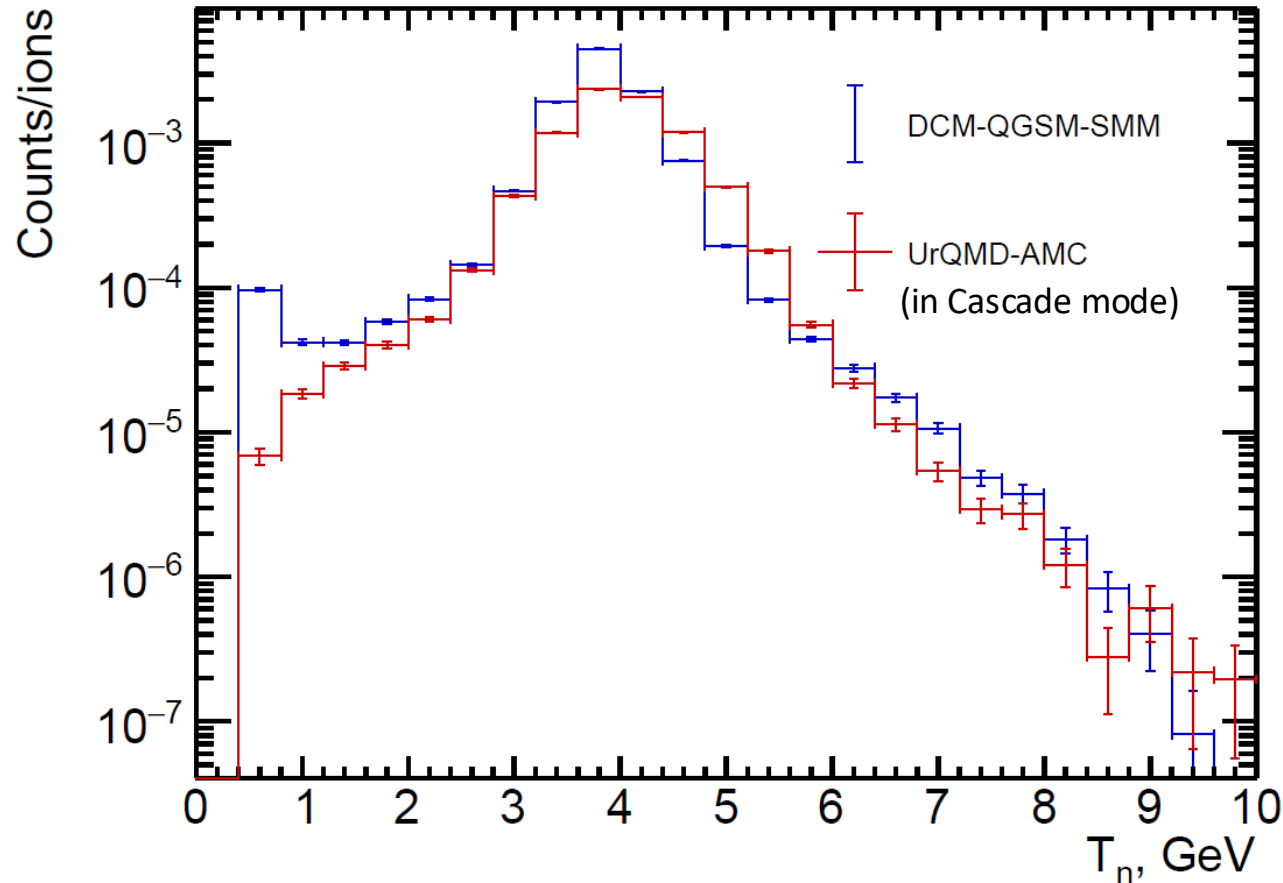


Spectator neutron multiplicity – **16.01**

Spectator neutrons on the surface of the HGND prototype

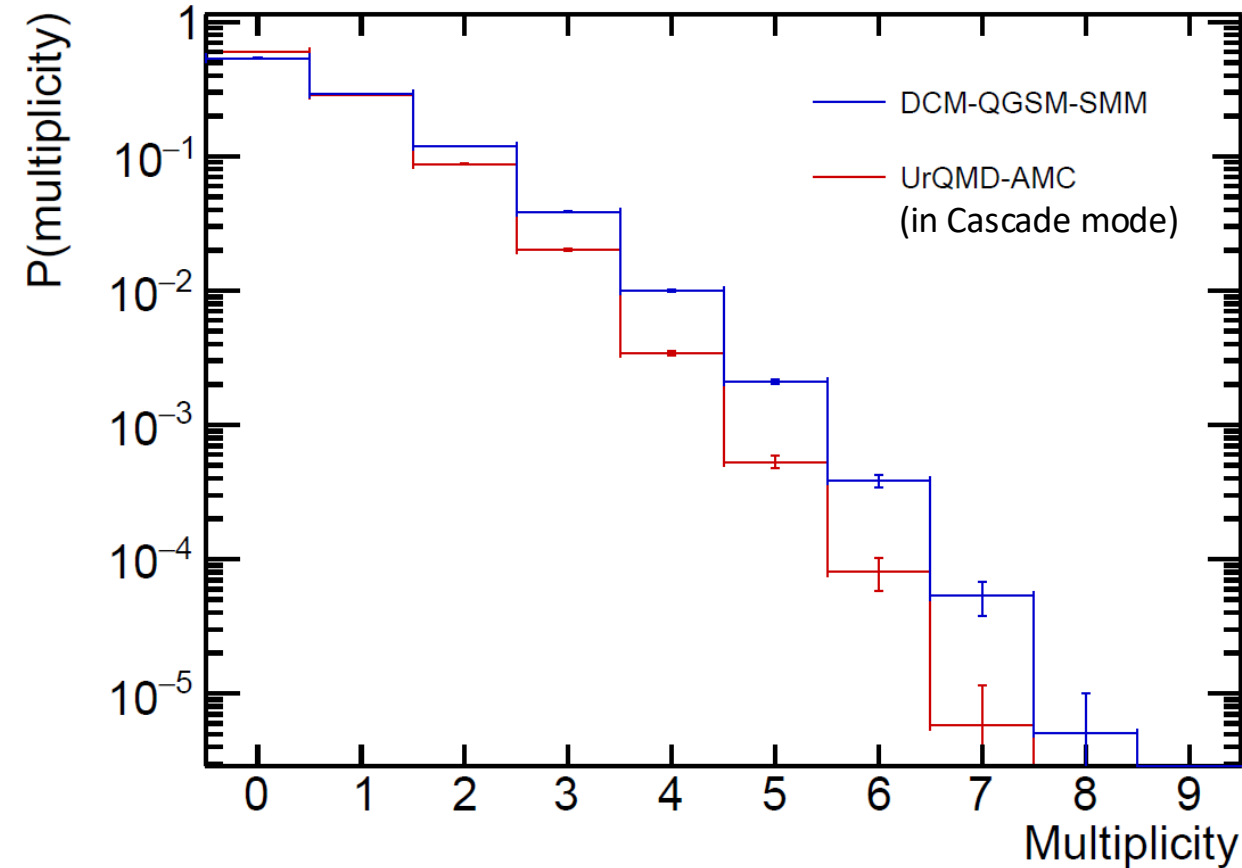


Neutron kinetic energy at the HGND prototype surface



Trigger efficiency correction from experimental data was applied for all histograms.

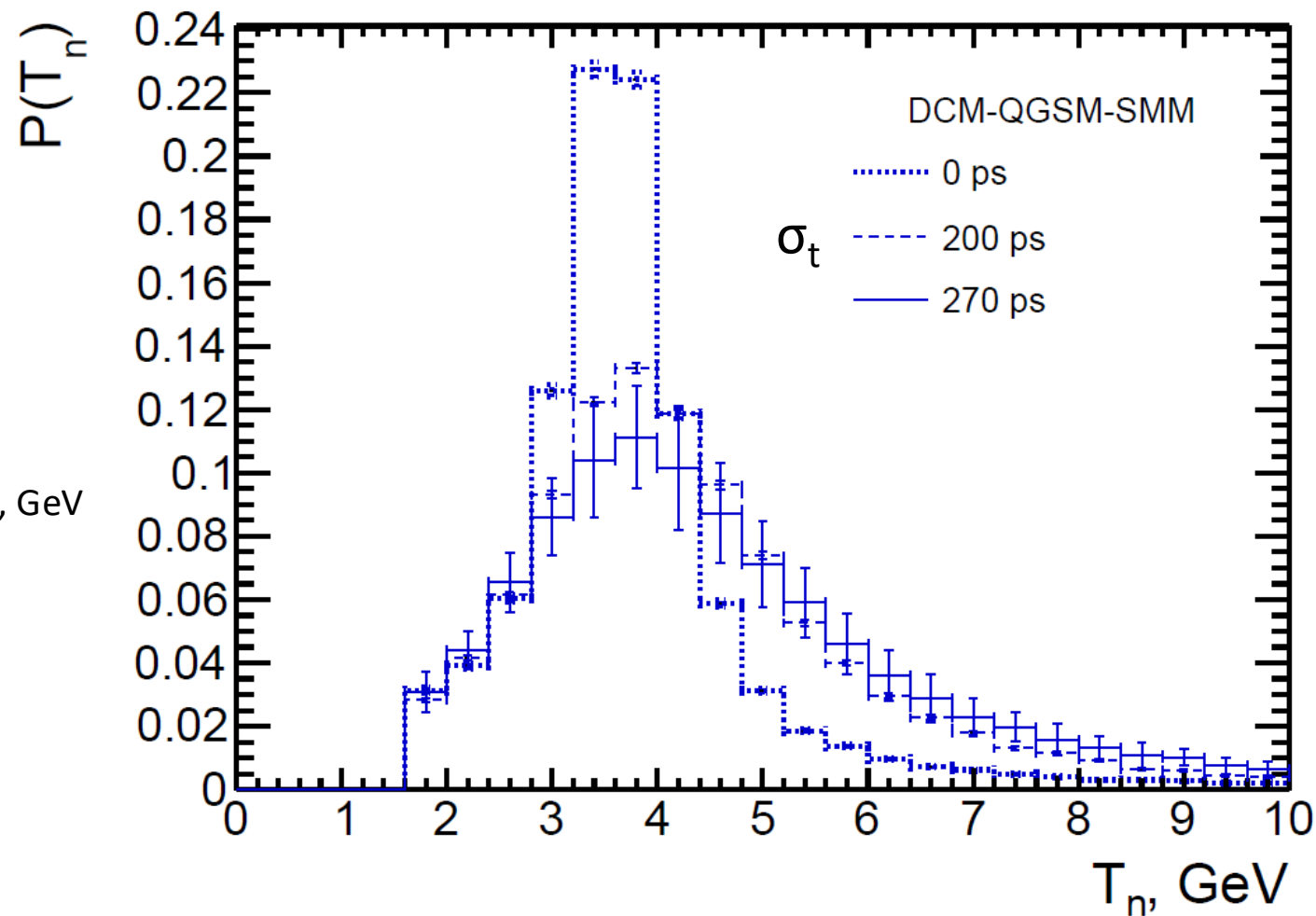
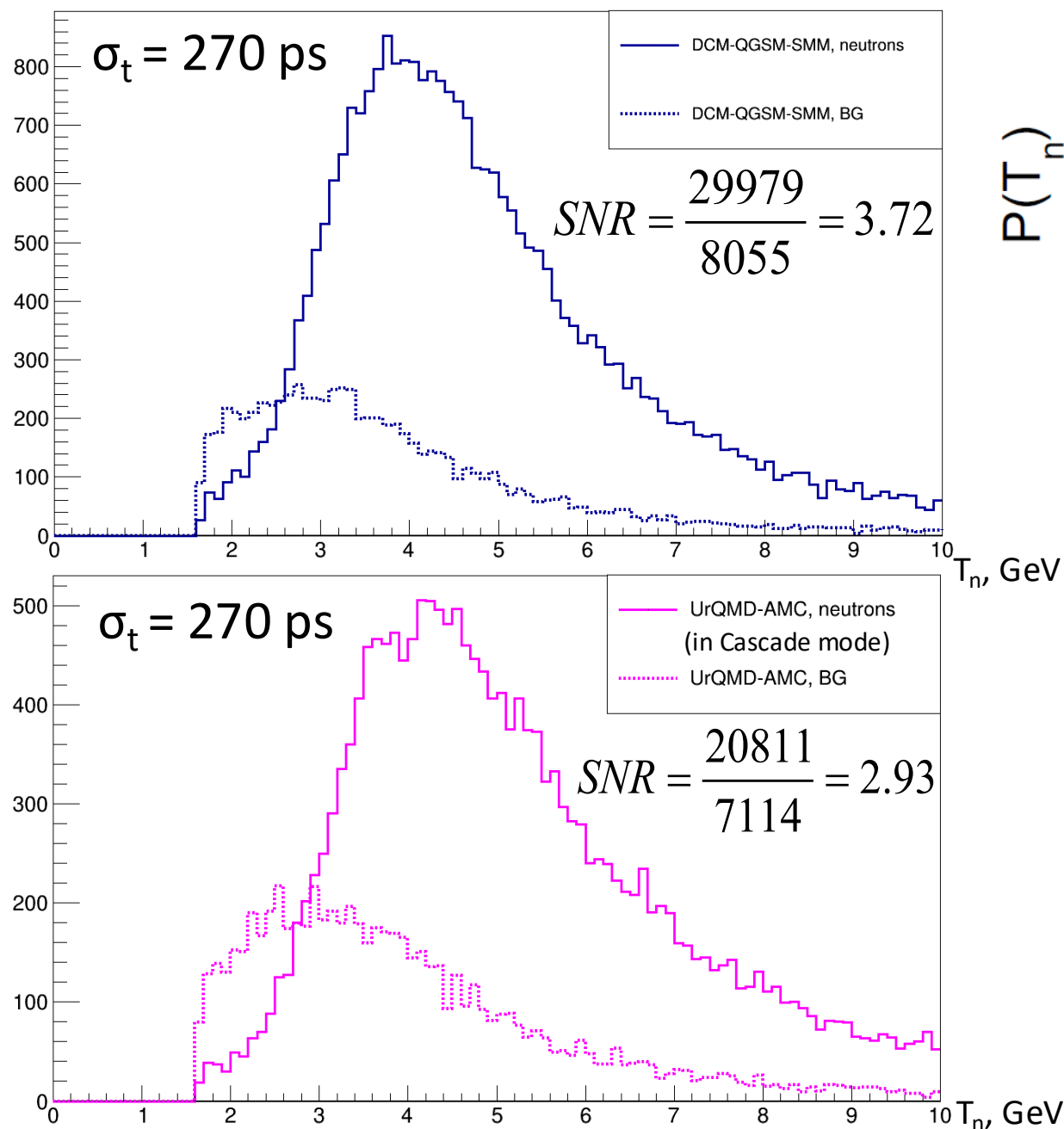
Neutron multiplicity at the HGND prototype surface

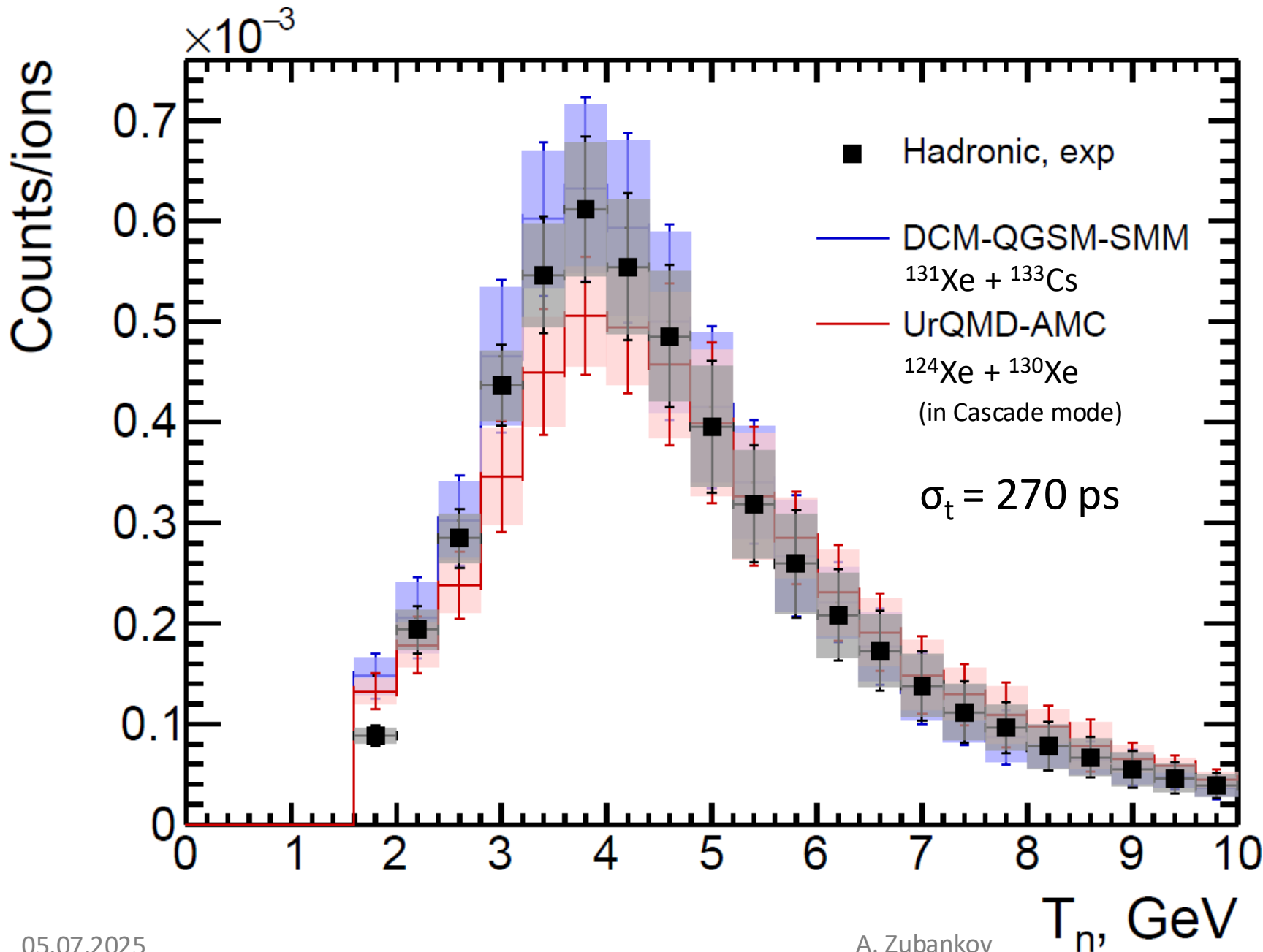


Neutron multiplicity hitting the surface of the HGND prototype

- **1.36** for **UrQMD-AMC (in Cascade mode)**
- **1.51** for **DCM-QGSM-SMM**

Backgrounds & time resolution for hadronic interactions





The difference in the shape and peak position of the reconstructed spectra of the models is noticeable, which is also due to the difference in the mean kinetic energy of neutrons and their multiplicity.

$$\Omega_n = \frac{N_{hit}}{N_{gen}} \quad \varepsilon_n = \frac{N_{rec}}{N_{hit}}$$

Model	Ω_n , %	ε_n , %	$\Omega_n \times \varepsilon_n$, %
DCM-QGSM-SMM	3.87 ± 0.02	37.33 ± 0.17	1.45 ± 0.01
UrQMD-AMC (in Cascade mode)	2.63 ± 0.01	45.09 ± 0.25	1.19 ± 0.01

The difference in Ω_n and ε_n is explained by the differences in angular distribution of primary neutrons (17.70 vs 16.01) and in average multiplicity of neutrons hitting the detector (1.36 vs 1.51).

4. Neutron yields and cross sections estimation

The sources of systematics are:

- The number of interactions per incident ion $\varepsilon_{ev/ions}$
- Source of trigger time ε_{time}
- Unevenness of the number of hits on HGND prototype modules $\varepsilon_{modules}$
- Uncertainty in the number of neutrons after photon rejection $\varepsilon_{\gamma-rejection}$

$$\Omega_n = \Omega_n^0 \cdot \varepsilon_{ev/ions}$$

$$\varepsilon_n = \varepsilon_n^0 \cdot \varepsilon_{time} \cdot \varepsilon_{modules} \cdot \varepsilon_{\gamma-rejection}$$

Source of systematics	EMD systematics RELDIS	Hadronic systematics	
		DCM-QGSM-SMM	UrQMD-AMC (in Cascade mode)
$\varepsilon_{ev/ions}$	-	1.60%	
ε_{time}	0.53%	0.36%	
$\varepsilon_{modules}$	2.36%	7.72%	1.47%
$\varepsilon_{\gamma-rejection}$	0.73%	1.58%	2.55%
Total	2.52%	8.05%	3.36%

Cross-section estimation using different models



$$\sigma = \frac{N_{ev} \cdot \langle N_n \rangle}{N_{ions}} \cdot \frac{A}{d \cdot N_A \cdot \rho} \cdot (\Omega_n \times \varepsilon_n)$$

$$d = 0.175 \text{ cm}$$

$$N_A = 6.02 \cdot 10^{23} \text{ mol}^{-1}$$

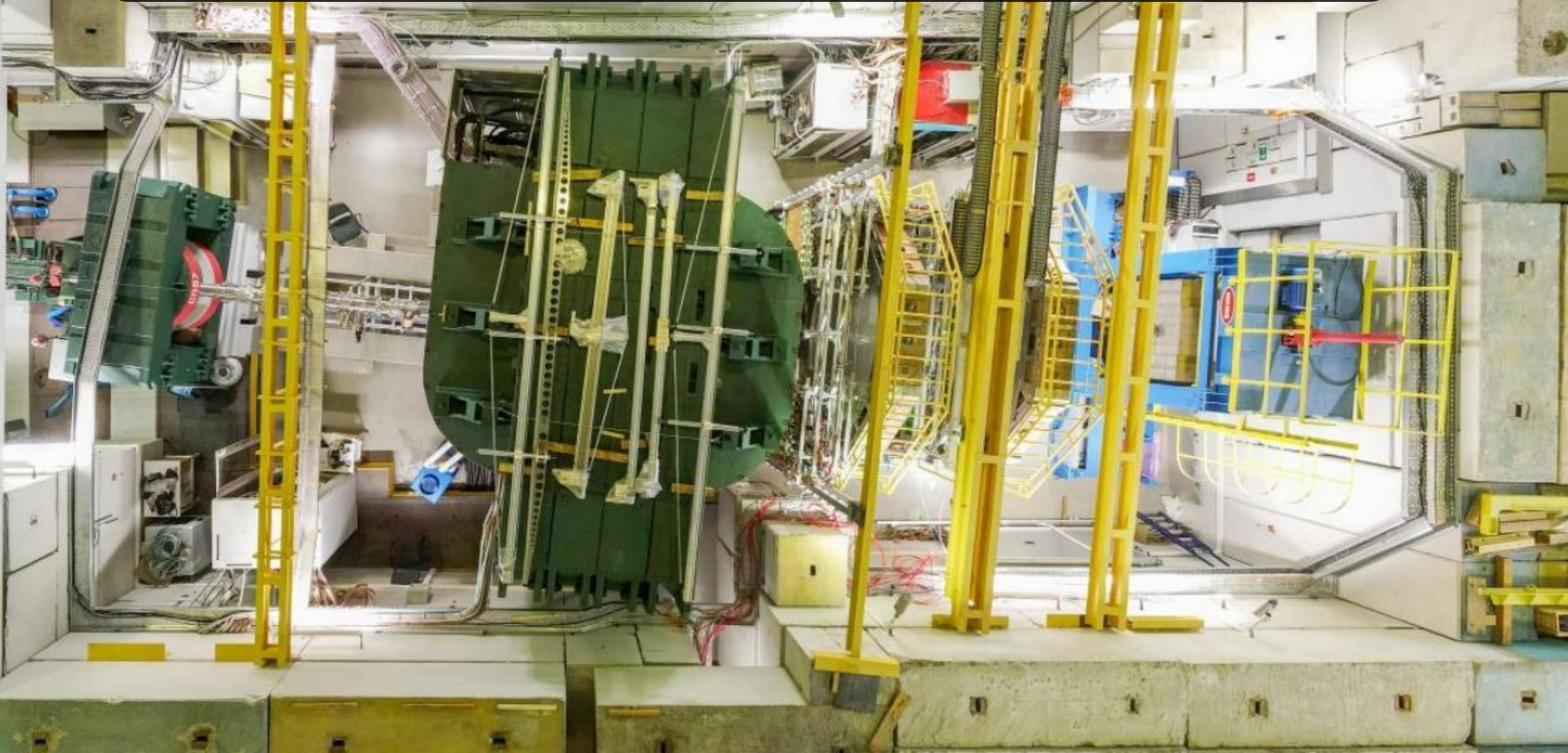
$$\rho = 4.53 \text{ g/cm}^3$$

	RELDIS	DCM-QGSM-SMM	UrQMD-AMC (in Cascade mode)
N_{ev} / N_{ions}	$(1.49 \pm 0.12) \cdot 10^{-3}$	$(3.78 \pm 0.02) \cdot 10^{-3}$	
$N_{ev} \cdot \langle N_n \rangle / N_{ions} \cdot (\Omega_n \times \varepsilon_n)$	$(6.92 \pm 0.57_{\text{stat}} \pm 0.17_{\text{syst}}) \cdot 10^{-3}$	$(16.31 \pm 0.10_{\text{stat}} \pm 1.31_{\text{syst}}) \cdot 10^{-3}$	$(17.98 \pm 0.13_{\text{stat}} \pm 0.60_{\text{syst}}) \cdot 10^{-3}$
σ^{exp}	$1.88 \pm 0.16_{\text{stat}} \pm 0.05_{\text{syst}} \text{ b}$	$4.44 \pm 0.03_{\text{stat}} \pm 0.36_{\text{syst}} \text{ b}$	$4.90 \pm 0.03_{\text{stat}} \pm 0.16_{\text{syst}} \text{ b}$
σ^{sim}	$1.89 \pm 0.02 \text{ b}$	$4.76 \pm 0.01 \text{ b}$	$4.89 \pm 0.01 \text{ b}$

Preliminary estimations are in good agreement within the errors with the modeling predictions.

- The acceptance and efficiency of the HGND prototype in detecting projectile spectator neutrons from hadronic interactions were studied using UrQMD-AMC (in Cascade mode) and DCM-QGSM-SMM models to generate primary collisions.
- The models were validated with GSI data on neutron production in 600A MeV $^{124}\text{Sn} + ^{124}\text{Sn}$ reaction.
- Also, efficiency and acceptance have been investigated for neutrons from EMD using the RELDIS model.
- Reconstructed spectra obtained with modeling are in good agreement within the errors with the experimental data.
- Preliminary estimates of neutron-spectators yields and cross sections have been made.
- See A. Shabanov's report on methods of background control in full-scale HGND.

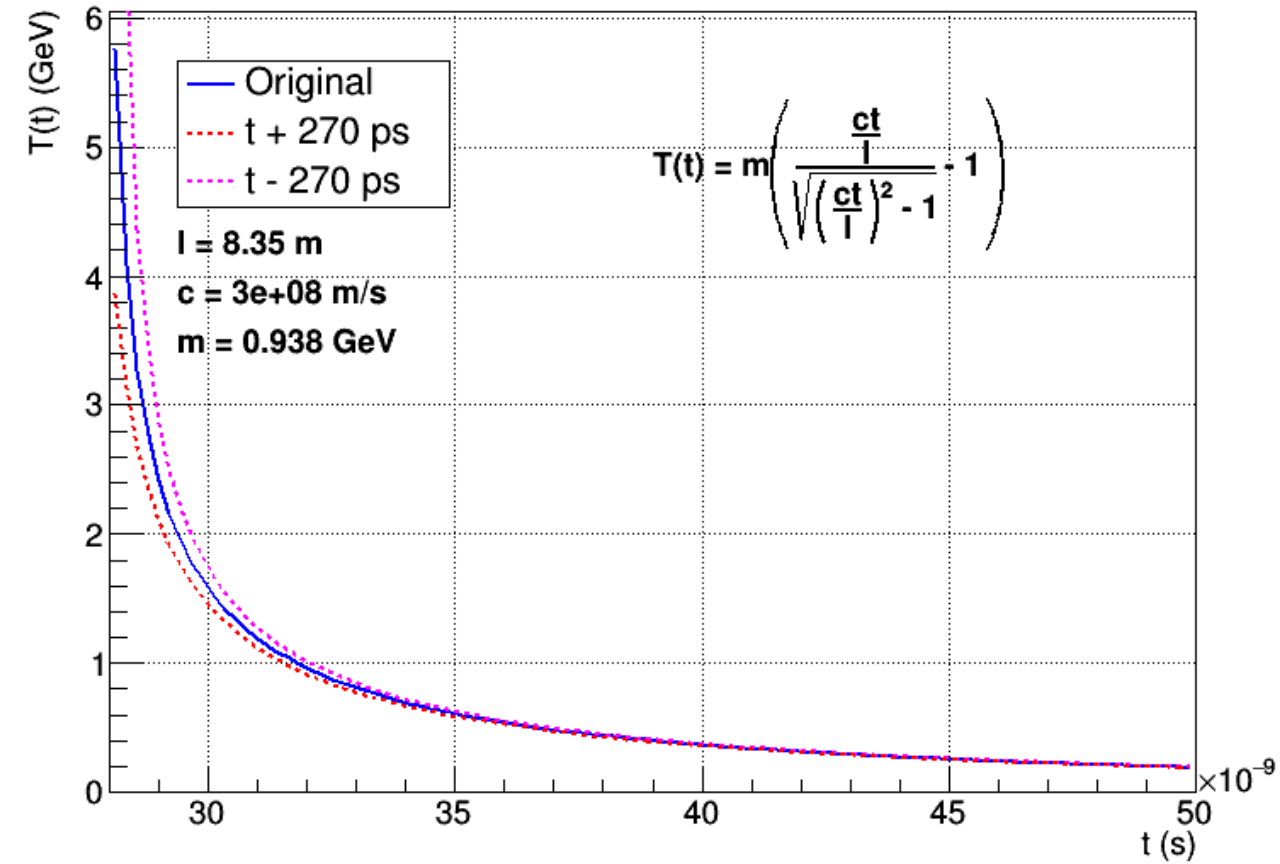
Thank you for your attention!



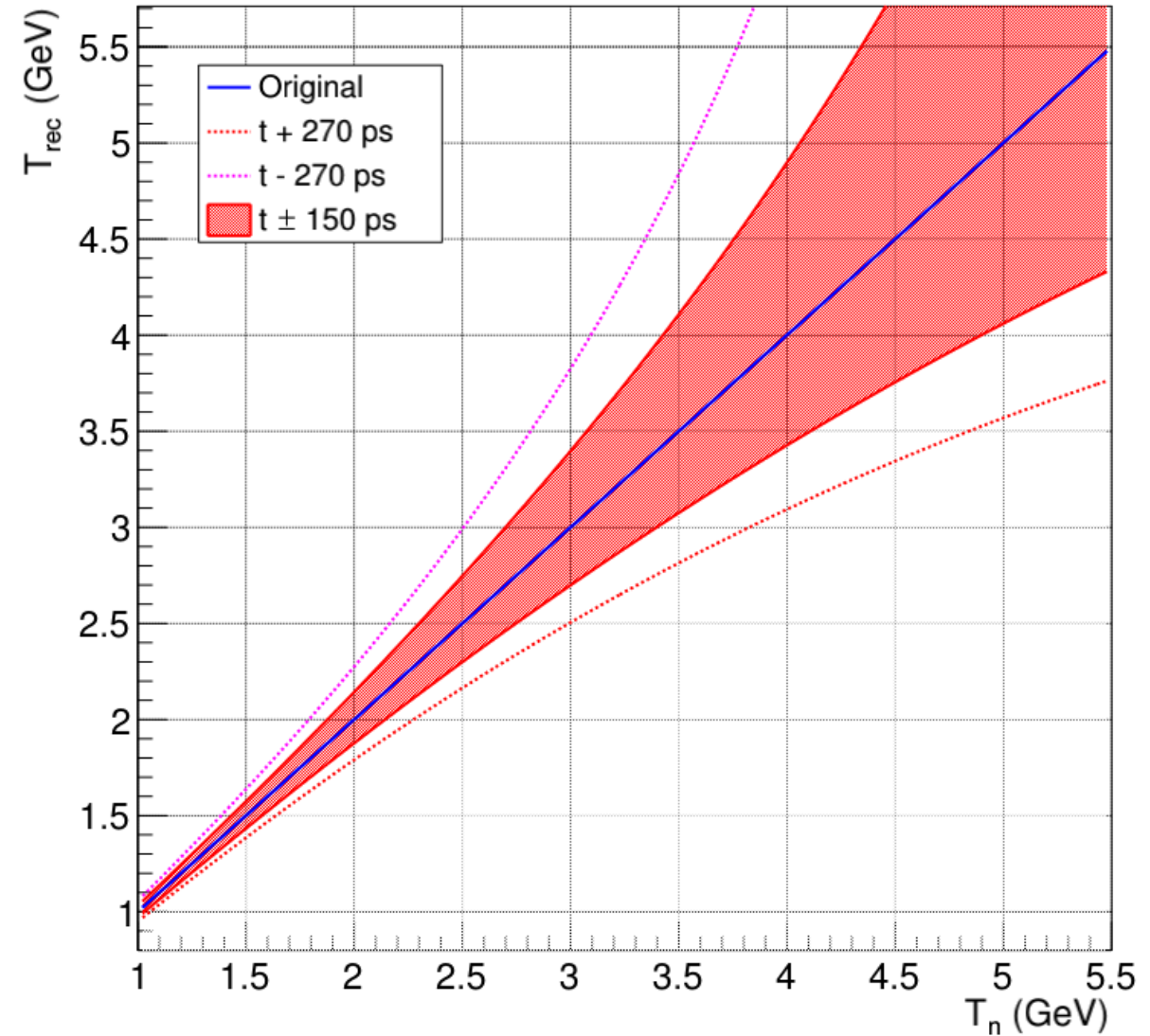
Backup

HGND prototype

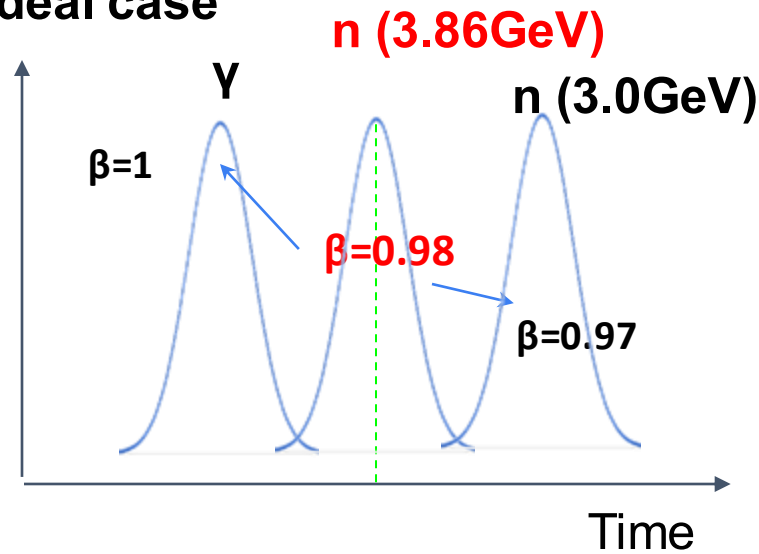
$T(t)$ vs t with ± 270 ps shift



T_{rec} vs T_n with ± 270 and 150 ps shifts

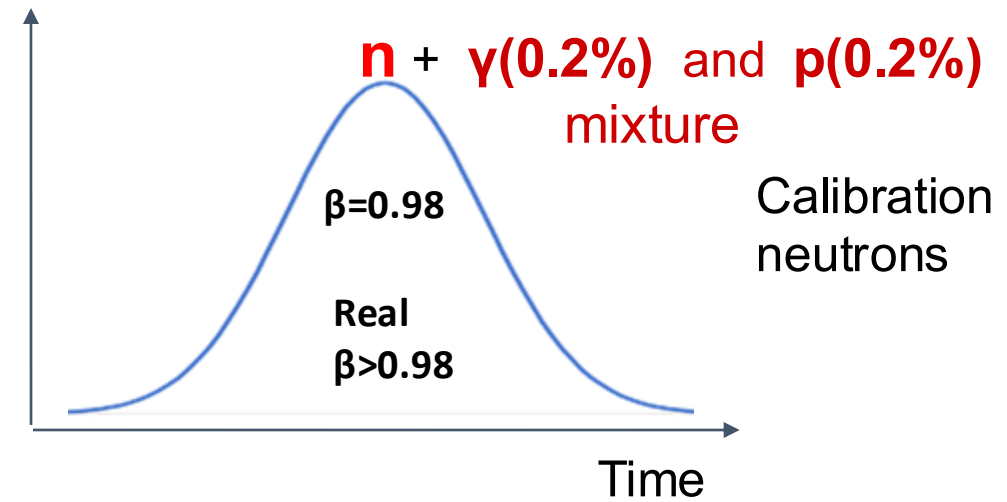


Ideal case

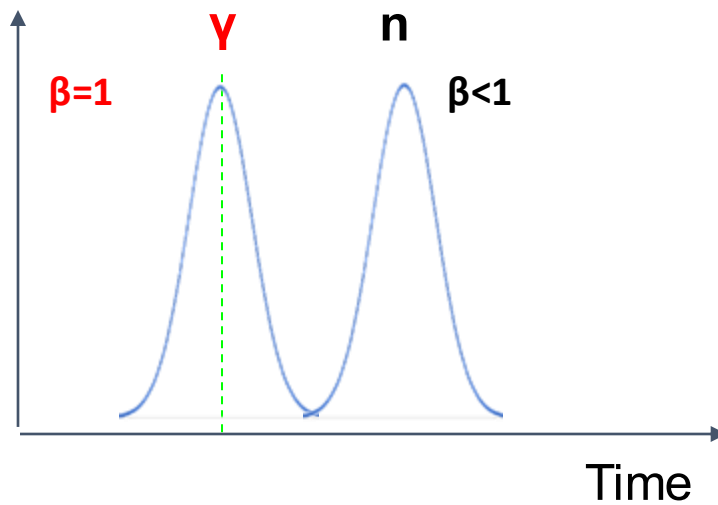


Calibration on neutrons

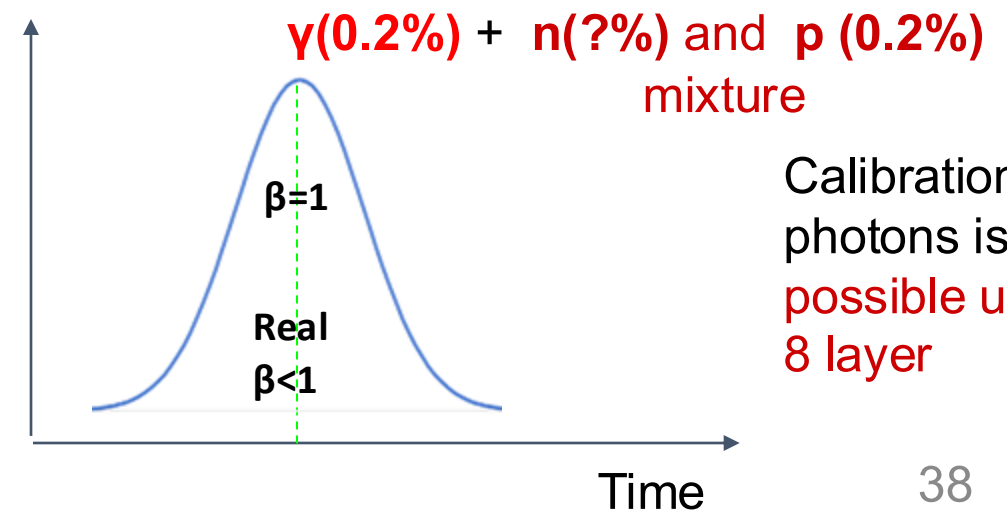
Real data



Calibration on neutrons



Calibration on photons

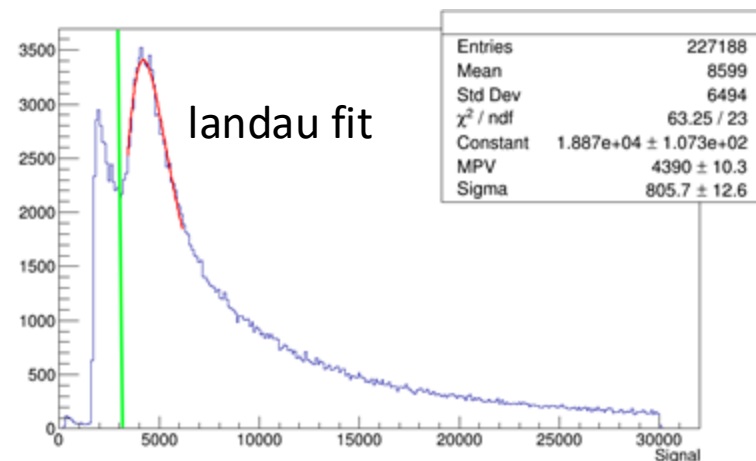


Calibration on photons is possible up to 8 layer

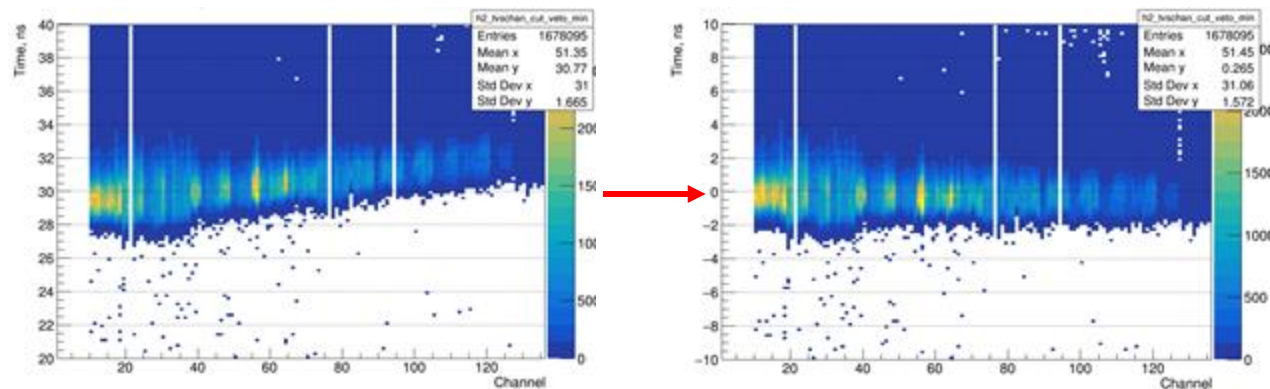
HGND calibration

1. Amplitude normalization

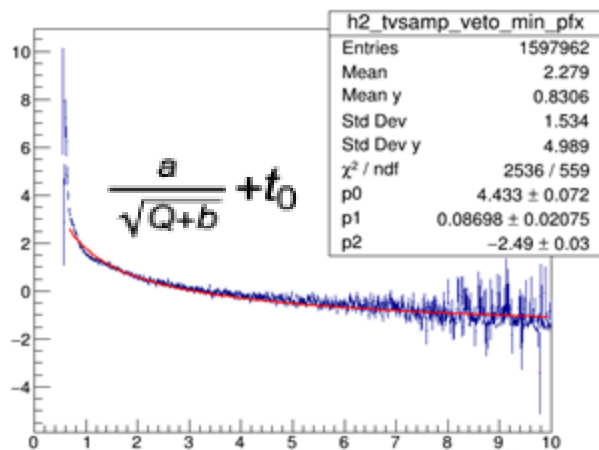
$$Ampl = Ampl \cdot \frac{1}{MPV}$$



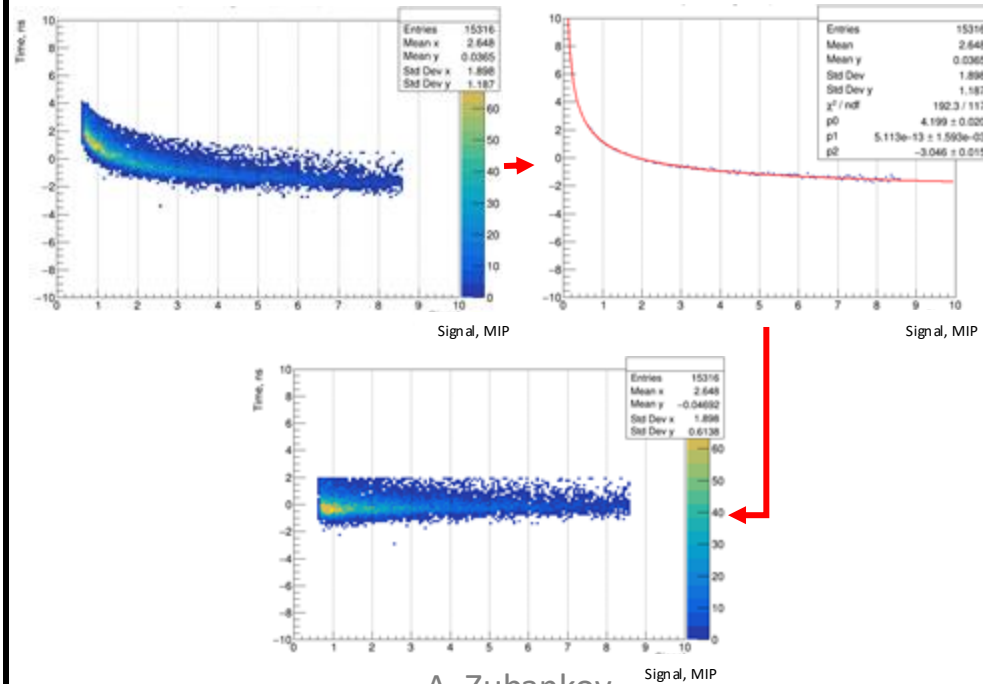
2. Time shift for all channels by the average fit value



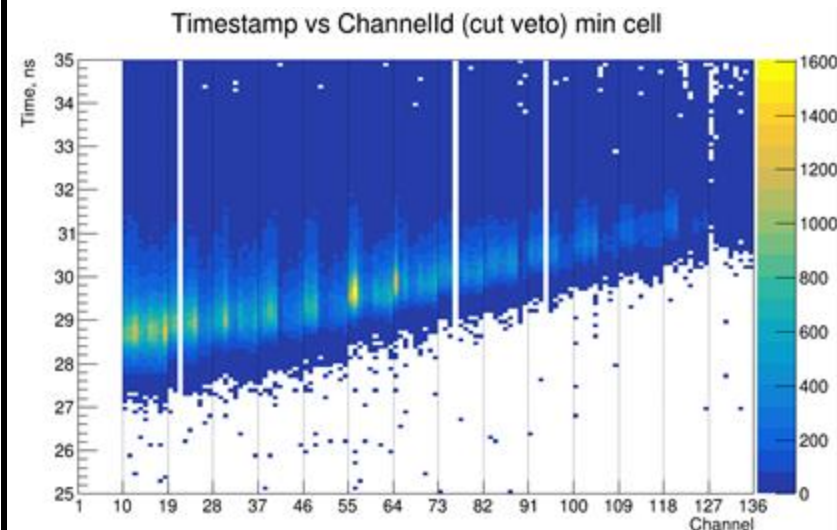
3. Determination of parameters of the approximating function for all channels & time limit



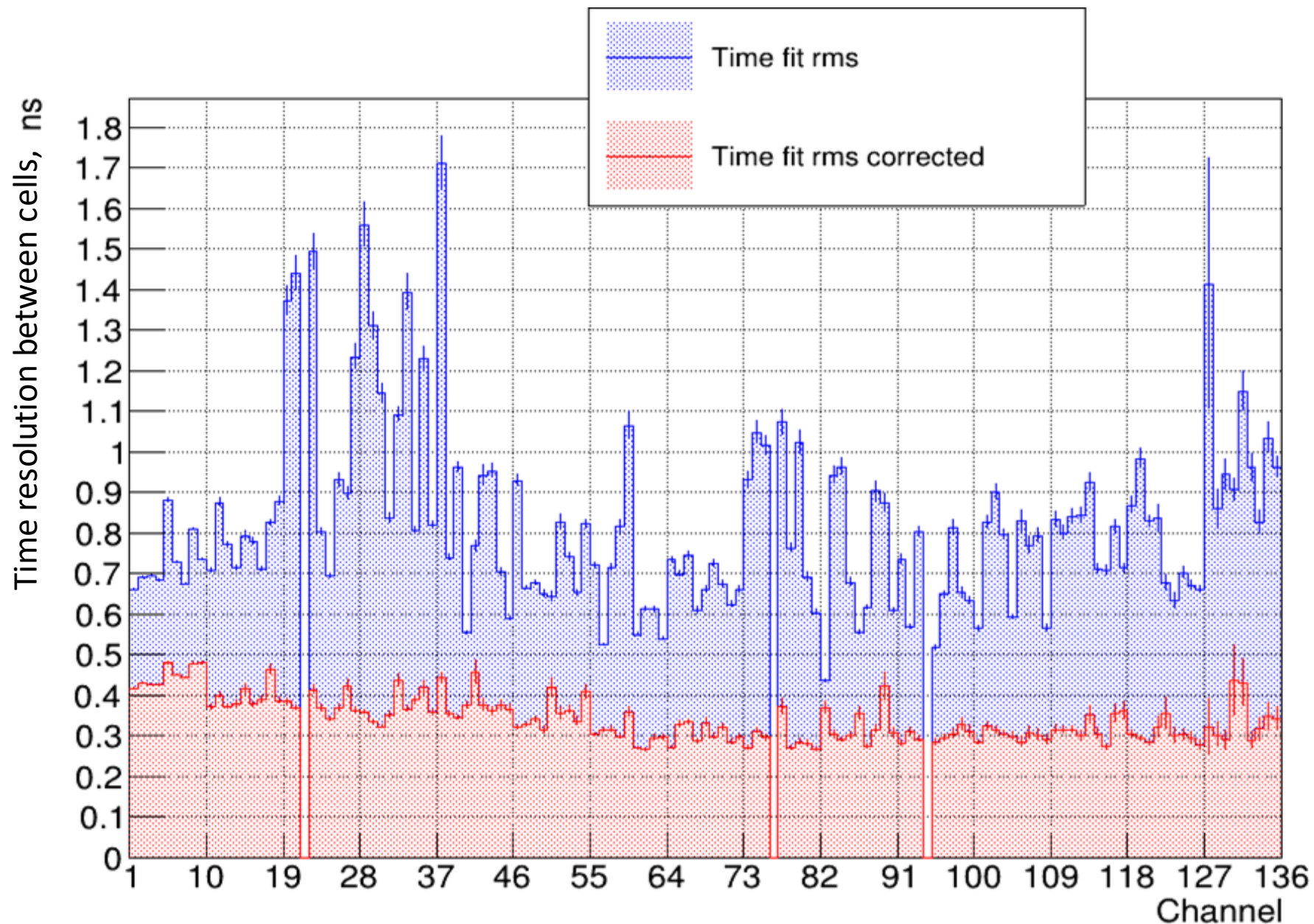
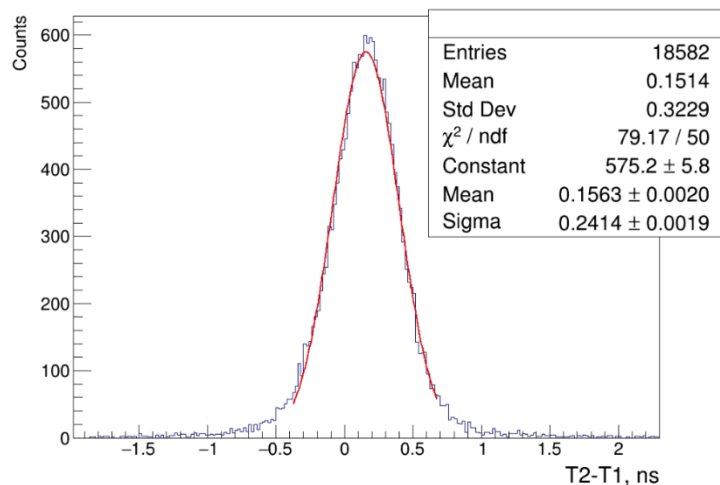
4. Time-amplitude correction



5. Time shift



Time-amplitude correction of signals made it possible to get rid of the dependence of time on signal amplitude, which improved the time resolution by ~ 2.4 times.

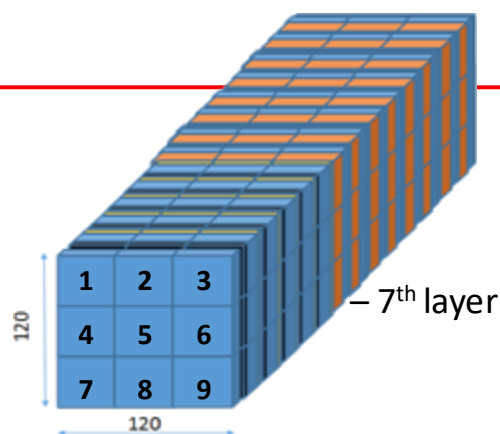
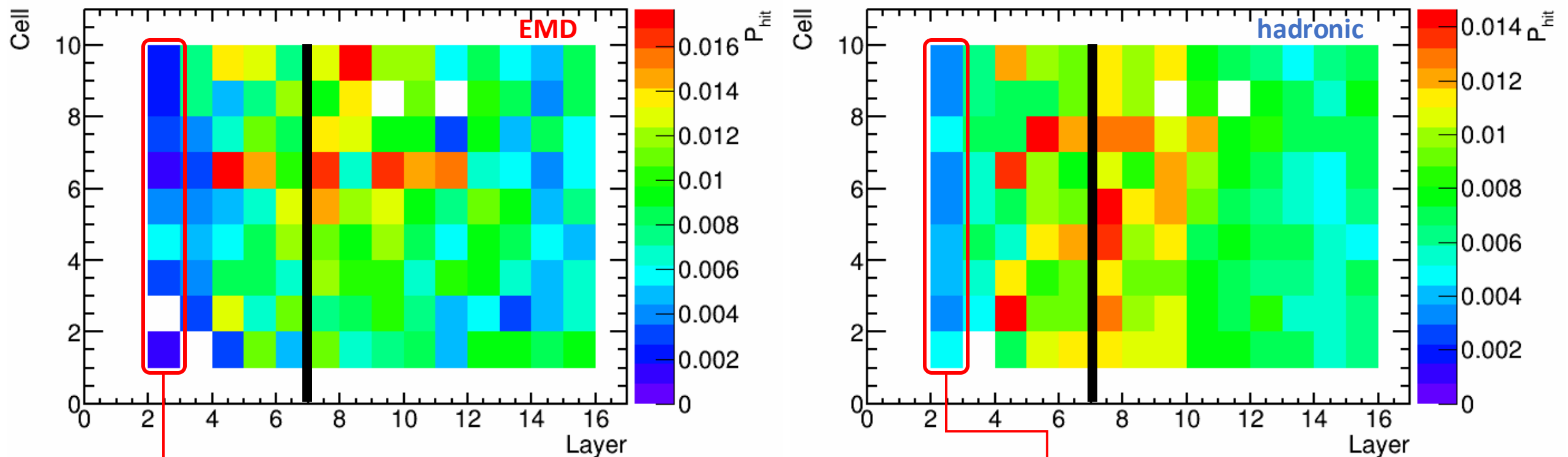


Fastest cells for EMD vs hadronic interactions



Comparison of hadronic interactions (CCT2) with electromagnetic dissociation (BT)

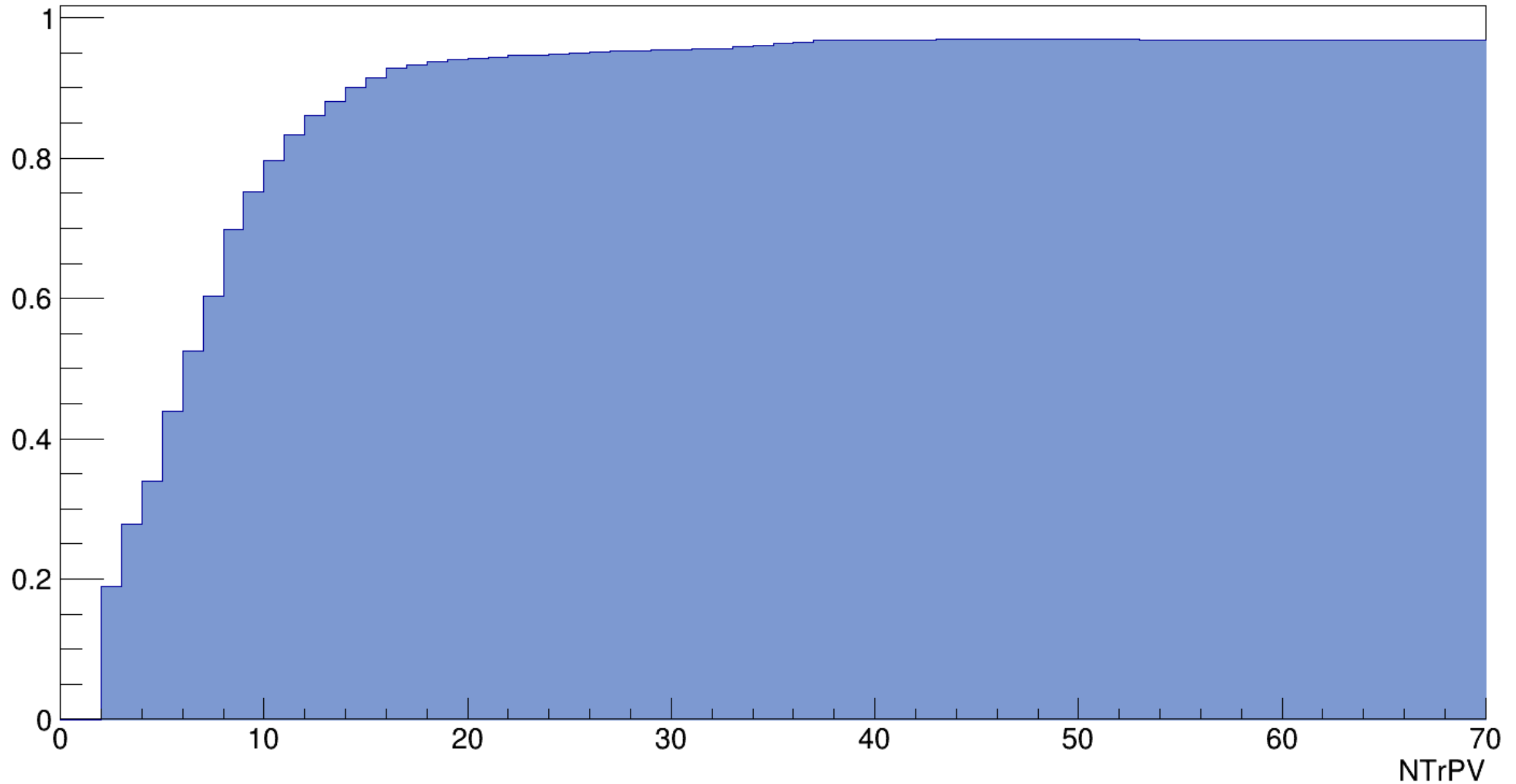
Run **8281 (BT)** vs **8300 (CCT2)** 3.8 AGeV

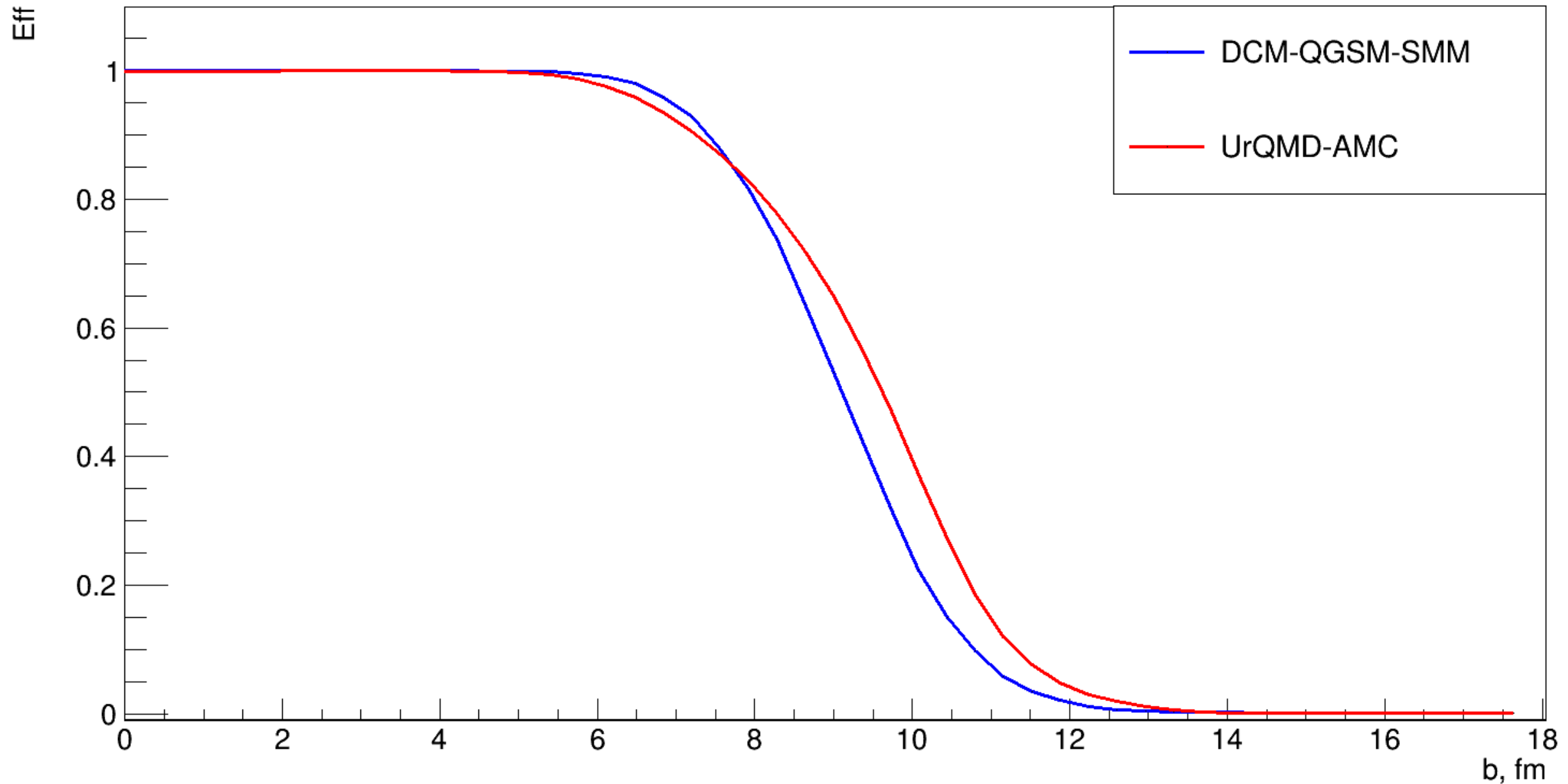


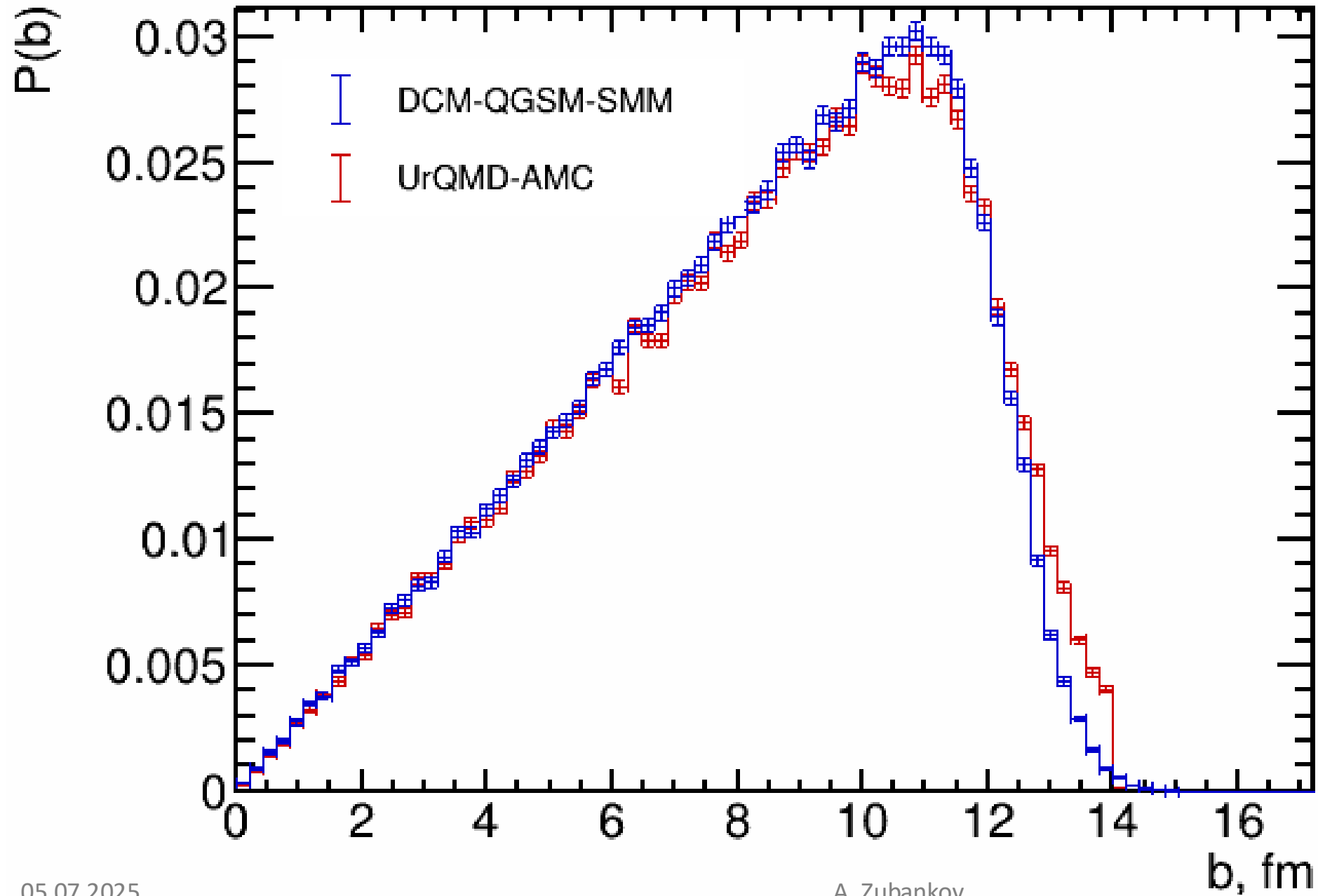
γ -quanta cut – no hits in 1-2 layers in module $\Rightarrow 1.55 X_0$ or $0.11 \lambda_{int}$

Most of the neutrons are deposited after the 7th layer for both EMD and nuclear interaction

Trigger efficiency







$$\begin{cases} P(d) = \frac{N_{ev} \cdot \langle N_n \rangle}{N_{ions}} \cdot (\Omega_n \times \varepsilon_n) \\ P(d) = 1 - \exp(-d/\lambda) \end{cases}$$

$$d = \lambda:$$

$$P(d) = \frac{d}{\lambda} = \frac{d \cdot N_A \cdot \rho \cdot \sigma}{A}$$

$$\sigma = \frac{N_{ev} \cdot \langle N_n \rangle}{N_{ions}} \cdot (\Omega_n \times \varepsilon_n) \cdot \frac{A}{d \cdot N_A \cdot \rho}$$

$$d = 0.175 \text{ cm}$$

$$N_A = 6.02 \cdot 10^{23} \text{ mol}^{-1}$$

$$\rho = 4.53 \text{ g/cm}^3$$

$$\Omega_n = \frac{N_{hit}}{N_{gen}} \quad \varepsilon_n = \frac{N_{rec}}{N_{hit}}$$

UrQMD-AMC

- The excited nuclear fragments are formed by means of MST-clusterization algorithm after UrQMD
 - A few excited nuclear prefragments can be formed, in contrast with DCM-QGSM-SMM, where all the spectator nucleon remain bound in one prefragment.
- Excitation energy of prefragment is calculated by hybrid approximation: a combination of Ericson formula for peripheral collisions and ALADIN approximation otherwise¹⁾
- Decays of prefragments are simulated as follows:
 - Fermi break-up model from Geant4 v9.2 ²⁾
 - Statistical Multifragmentation Model (SMM) from Geant4 v10.4 ²⁾
 - Weisskopf-Ewing evaporation model from Geant4 v10.4 ²⁾
- They were validated and adjusted to describe the data³⁾.

1) R. Nepeivoda, et al., Particles **5** (2022) 40

2) J. Alison et al. Nucl. Inst. A **835** (2016) 186

3) 55th Geant4 Technical Forum

<https://indico.cern.ch/event/1106118/contributions/4693132/>

- AMC is developed to simulate secondary decays of spectator fragments created in other models, in particular UrQMD.
- It is assumed that spectator matter is formed out of nucleons that do not undergo any collisions.

UrQMD:

- Version 3.4
- Cascade mode in this work
- Offset radius 5 fm
- Evolution time – 100 fm/c
- Other parameters are set to default values



Unigen file

AMC:

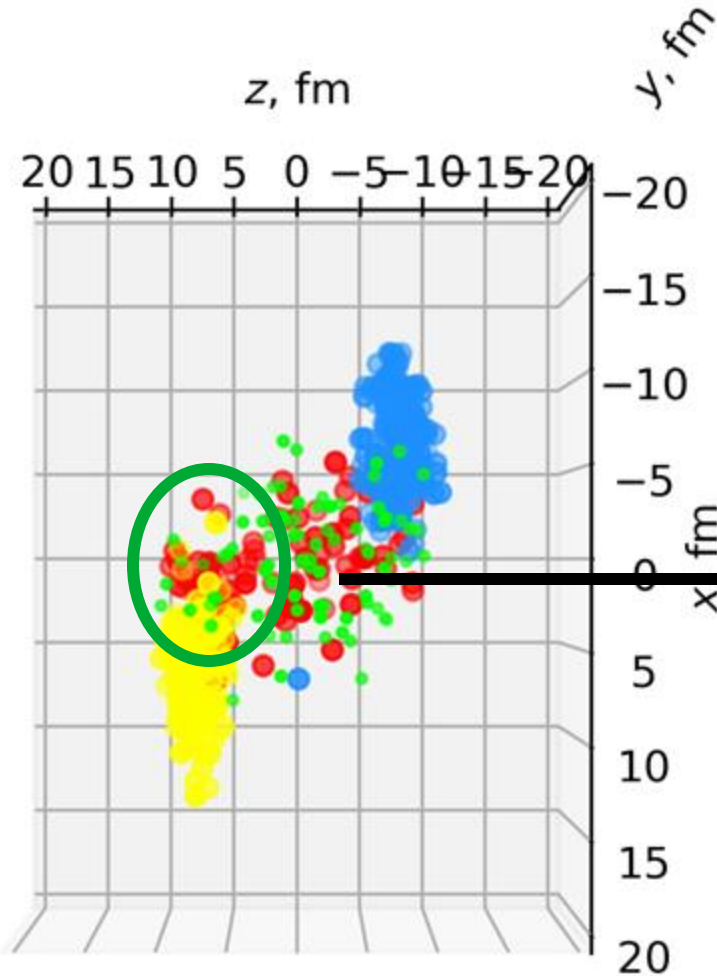
- Find spectator nucleons
- Define prefragments via MST-clustering
- Constant $d = 2.7$ fm
- Model prefragments decays
- All the participant data remain intact



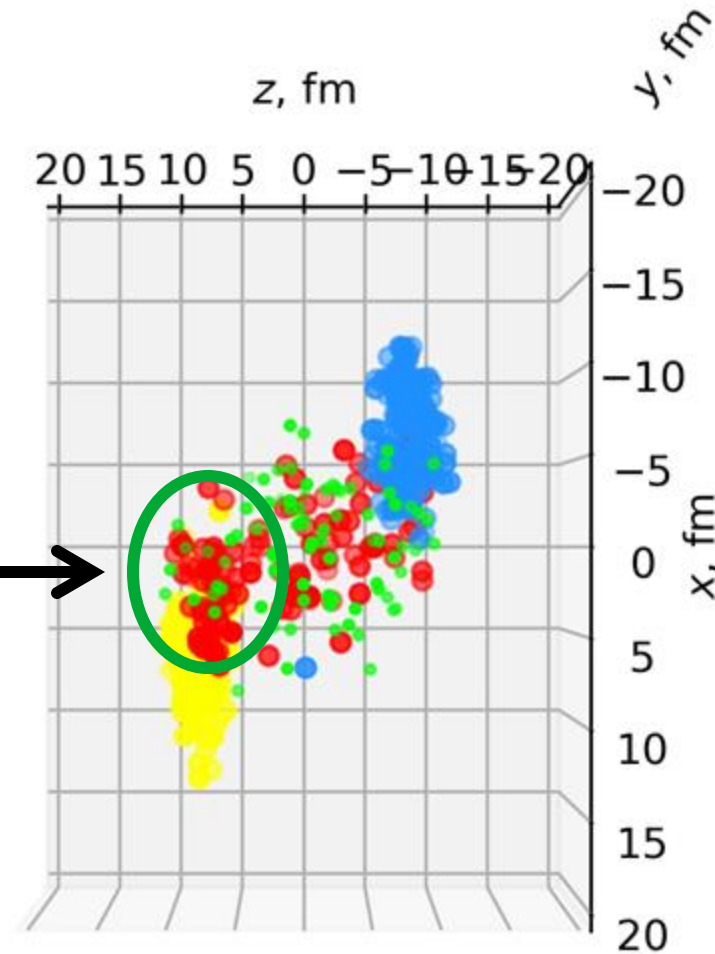
Unigen file

Knocking out some spectator nucleons by mesons

$b = 10 \text{ fm}$, $\tau = 13.5 \text{ fm}/c$

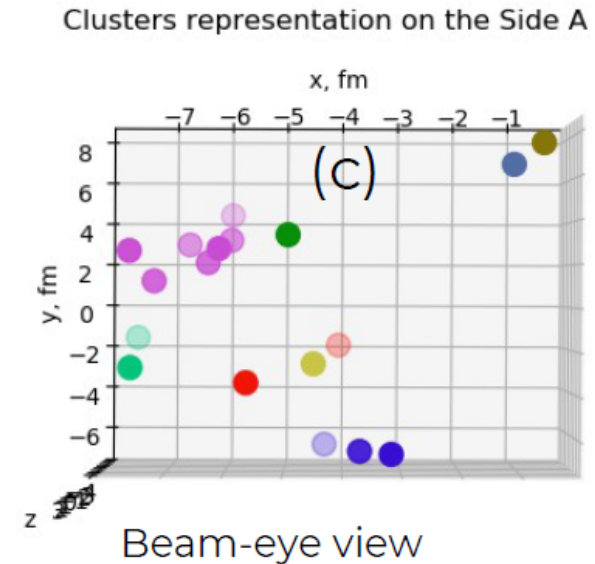
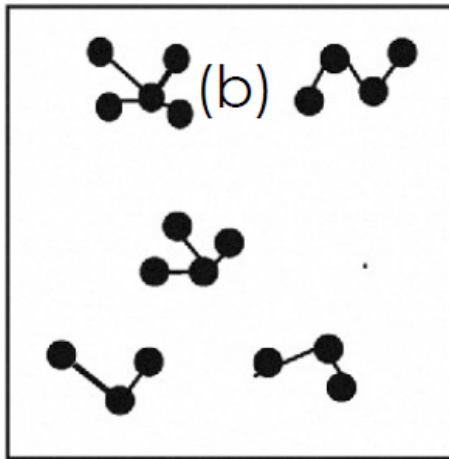
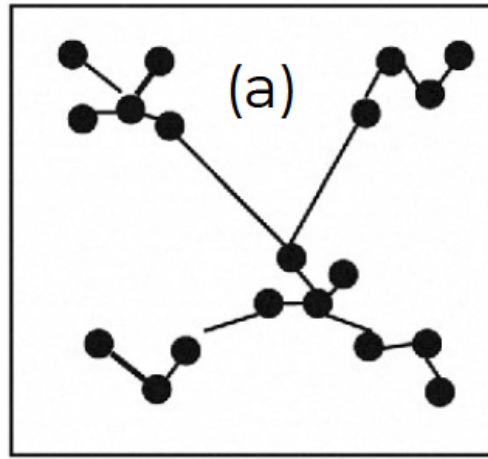


$b = 10 \text{ fm}$, $\tau = 14.0 \text{ fm}/c$

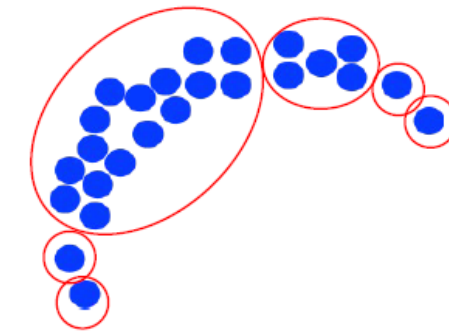


Blue and yellow – spectator nucleons, red – participant nucleons, green – produced mesons

MST-clustering



- Graph vertexes – nucleons, edges weights – Cartesian distances between them.
- **(a)** The minimum spanning tree is selected from the complete graph
- **(b)** All edges with a weight greater than d are removed. d is the clustering parameter depending on the excitation energy
- **(c)** Connectivity components are separate (pre-)fragments

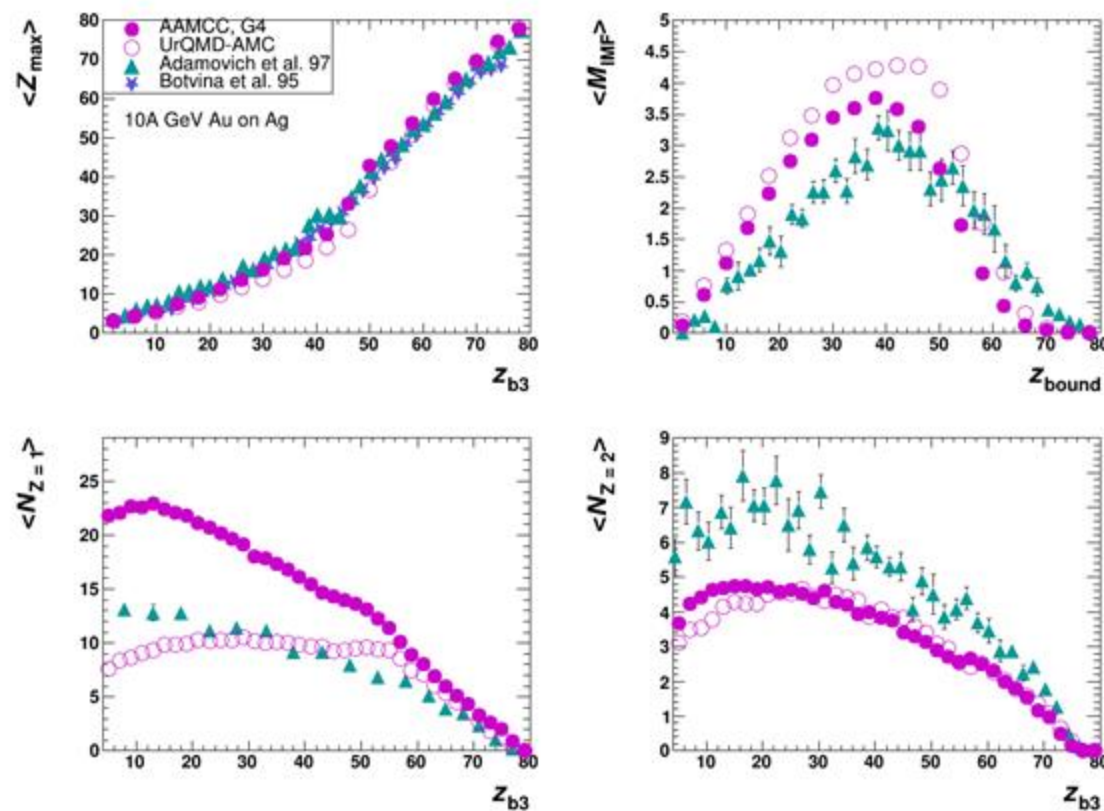


Prefragments in a central collision



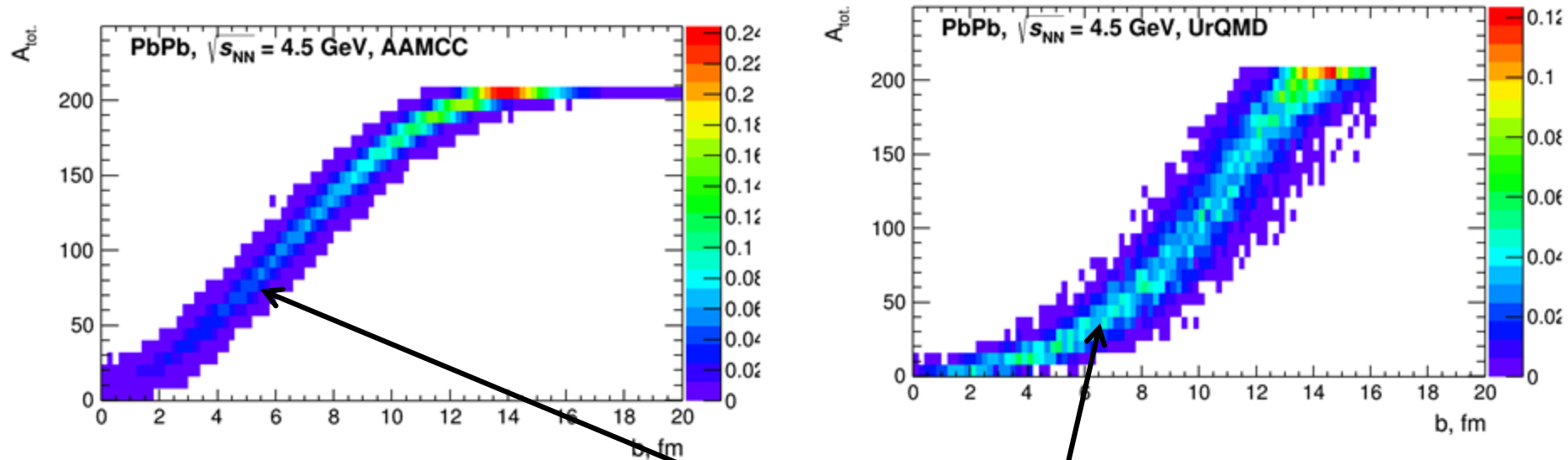
The prefragment is dynamically divided into several prefragments until thermodynamic equilibrium is reached.

^{197}Au fragmentation

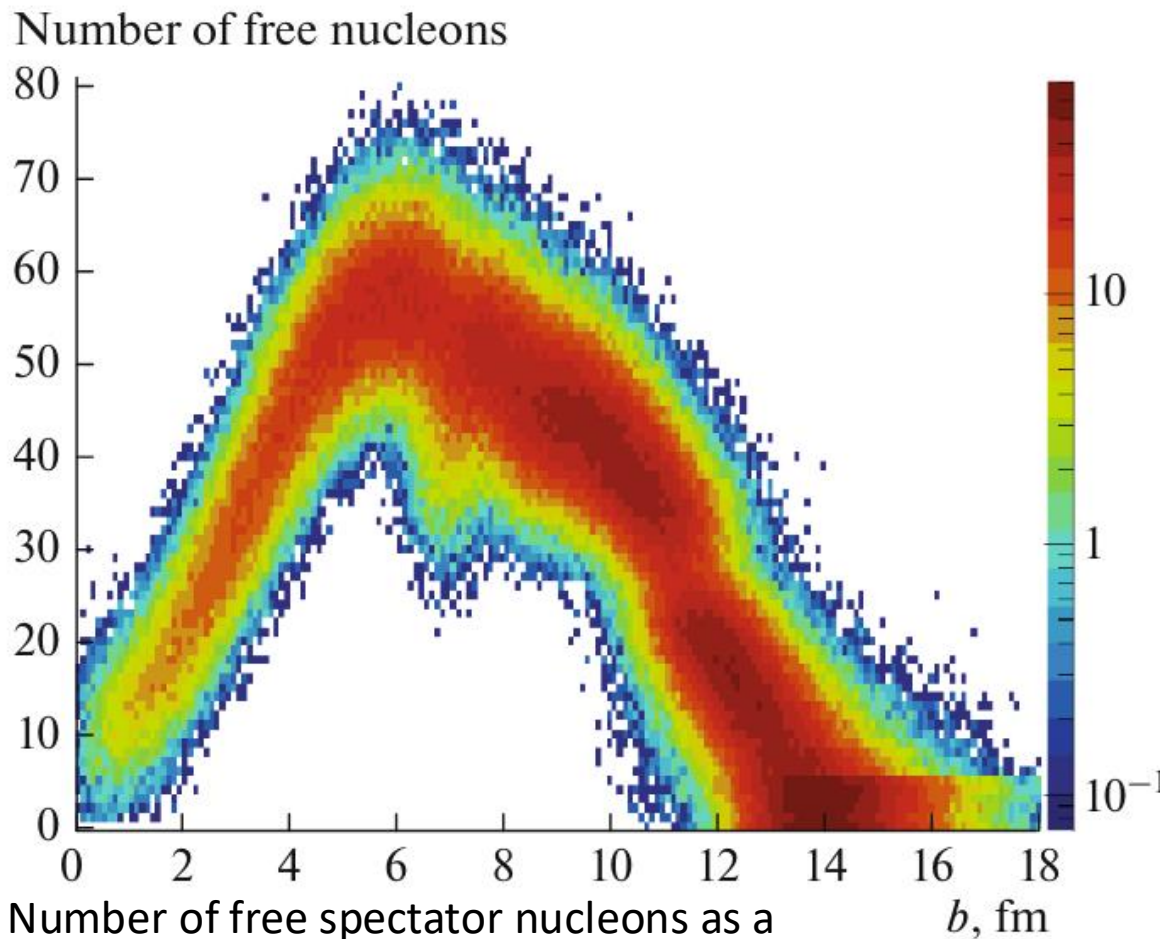


- UrQMD-AMC and AAMCC describe Z_{\max} . Models give similar numbers of He
- UrQMD-AMC is systematically lower than AAMCC for $Z_{\text{bound}} < 50$. This is due to a smaller spectator volume in UrQMD.
- AAMCC is closer to data on M_{IMF} , while UrQMD-AMC overestimates M_{IMF} in semi-central collisions. This is because of higher excitation energy of prefragments since more nucleons are removed.
- The difference in H fragments can be attributed to the different number of participants, because of a larger contribution of protons from MST-clustering

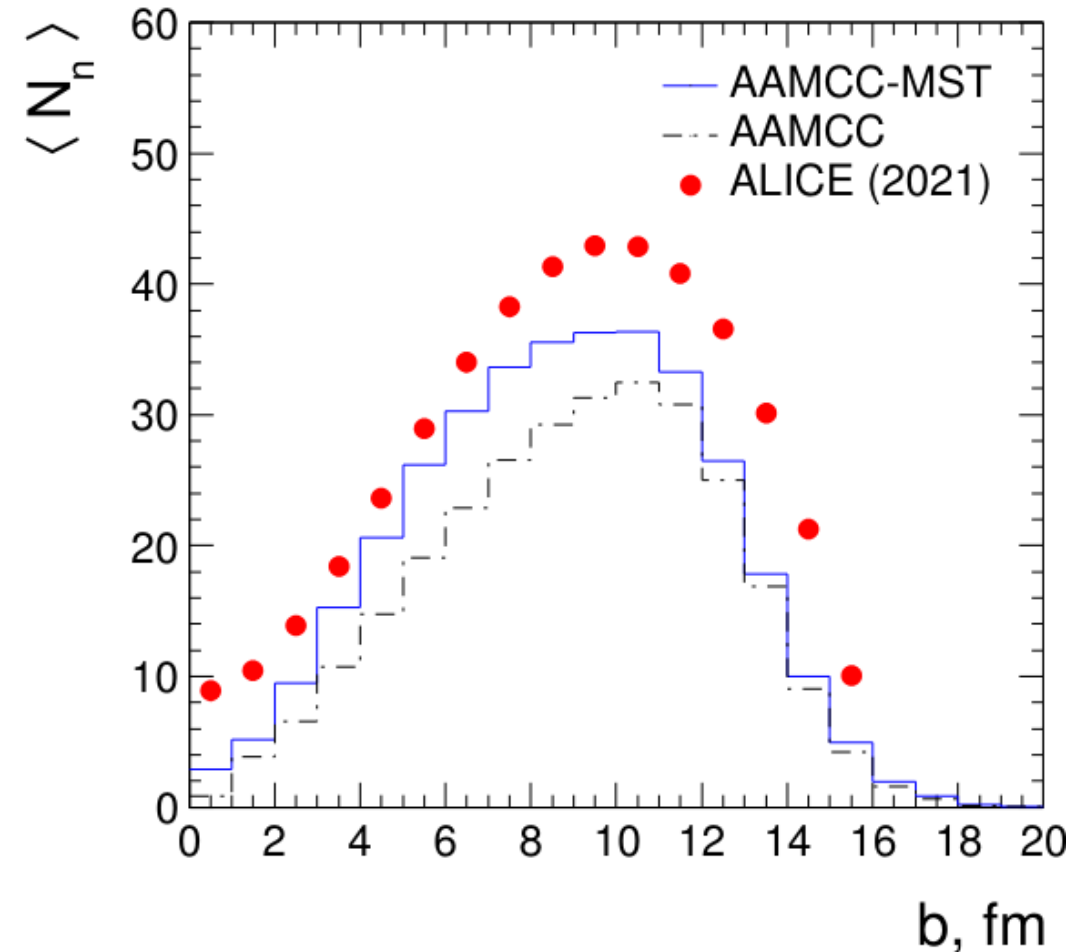
Spectator matter volume as a function of impact parameter



UrQMD gives less spectators than AAMCC for all b

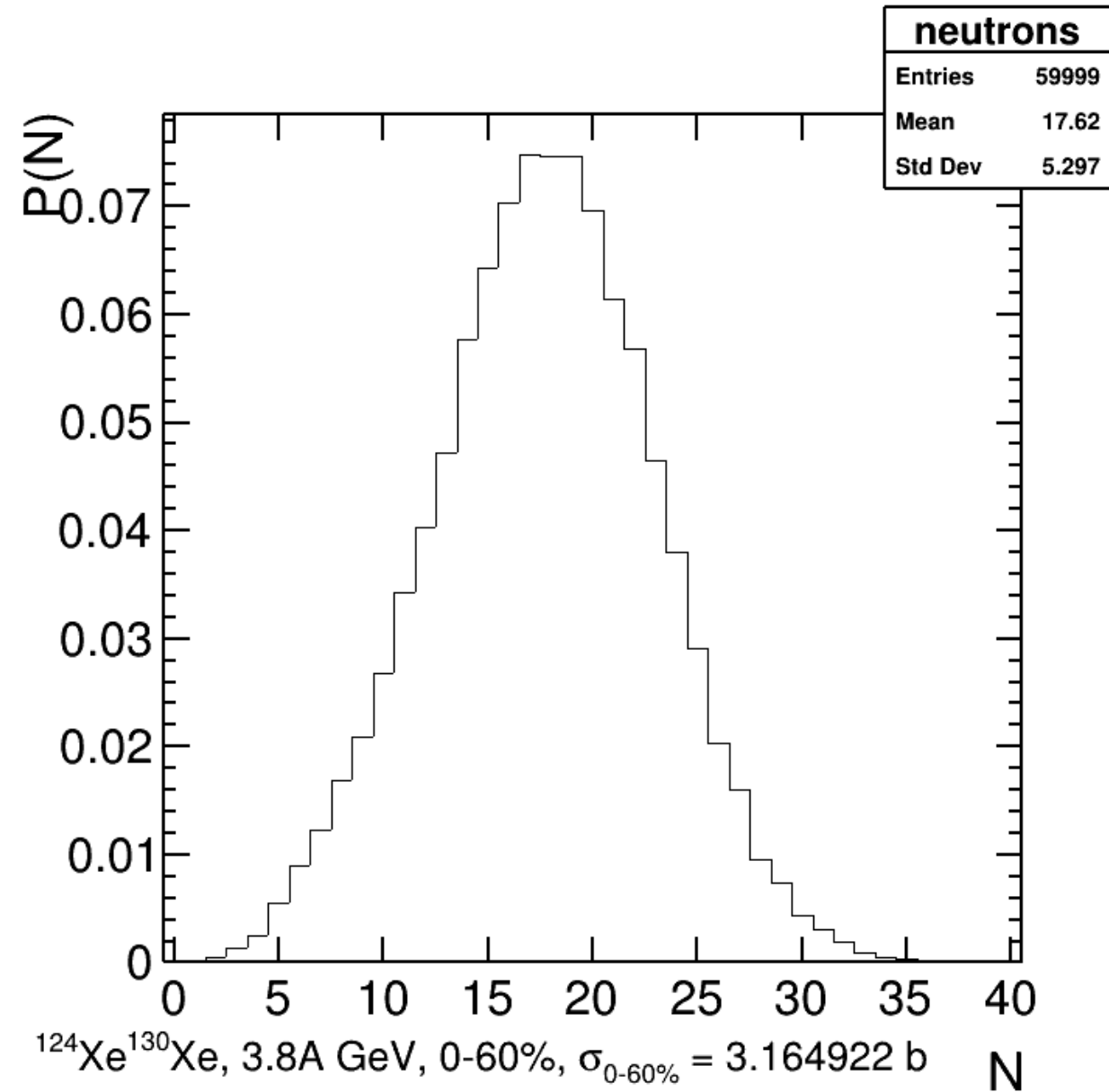
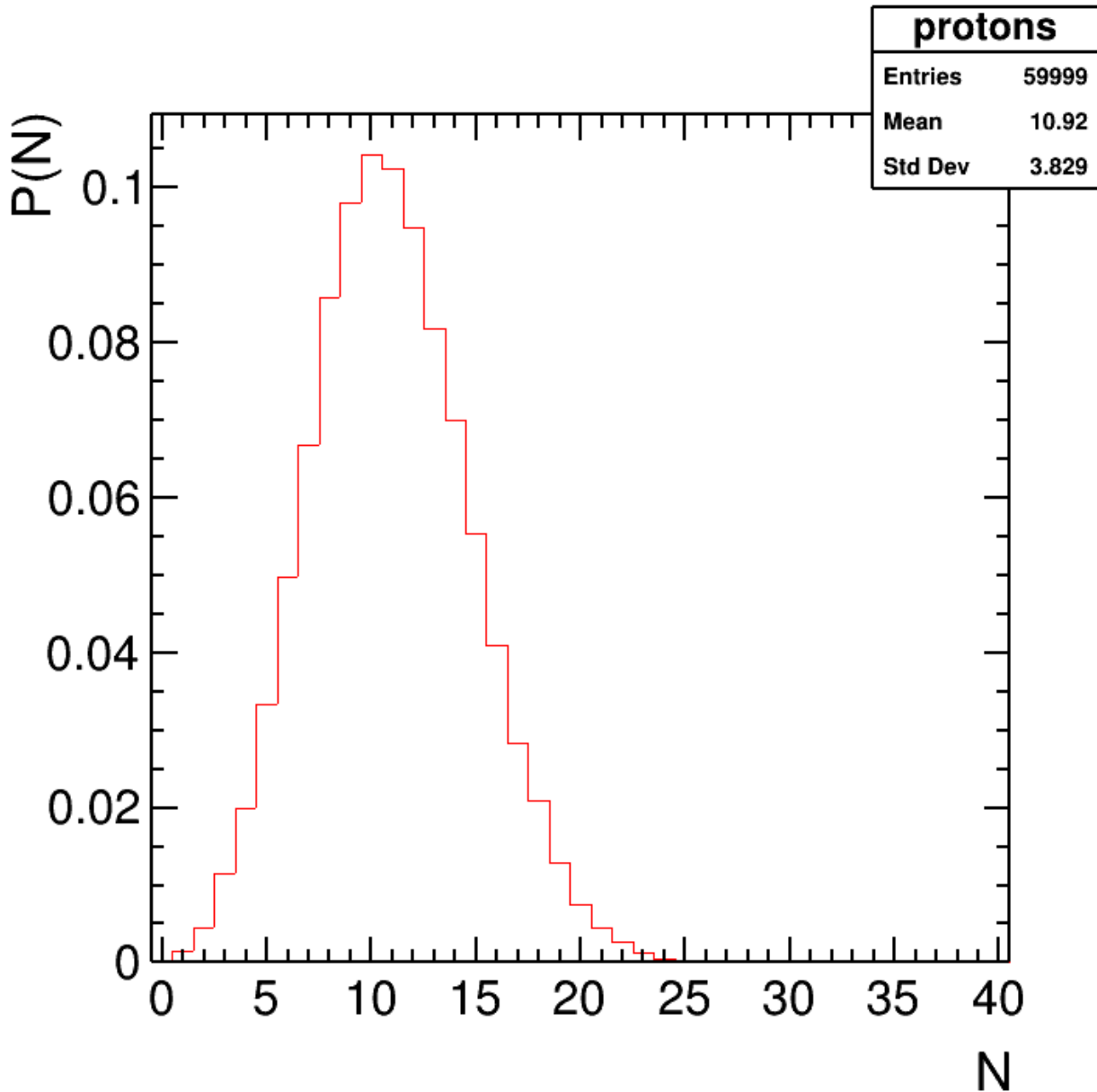


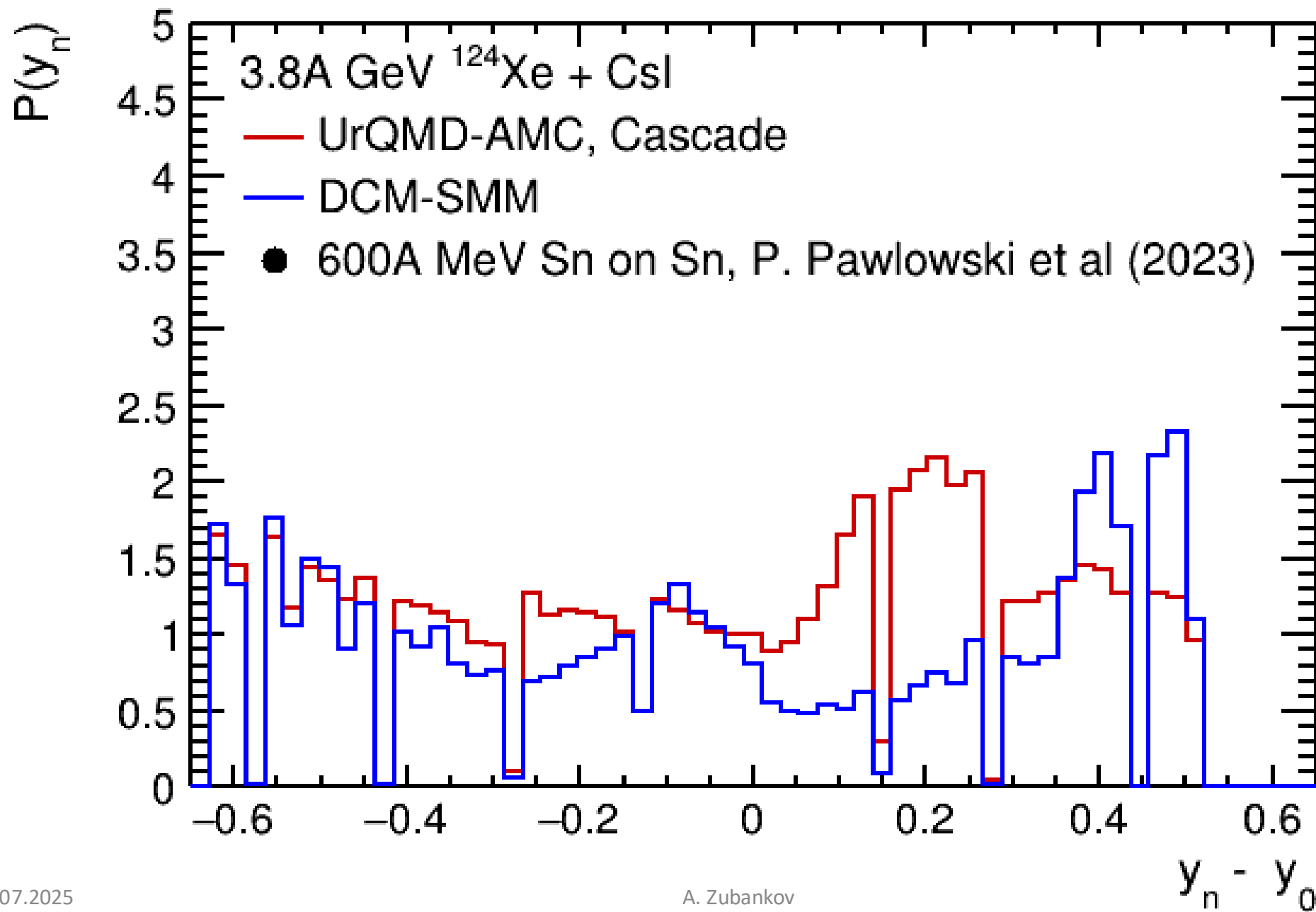
A. Svetlichnyi & I. Pshenichnov, Formation of Free and Bound Spectator Nucleons in Hadronic Interactions between Relativistic Nuclei. *Bulletin of the Russian Academy of Sciences: Physics* **2020**, 84 (8), 911–916.



Average multiplicities of neutrons in ^{208}Pb – ^{208}Pb collisions at $v_{\text{NN}} = 5.02$ TeV as functions of the collision impact parameter

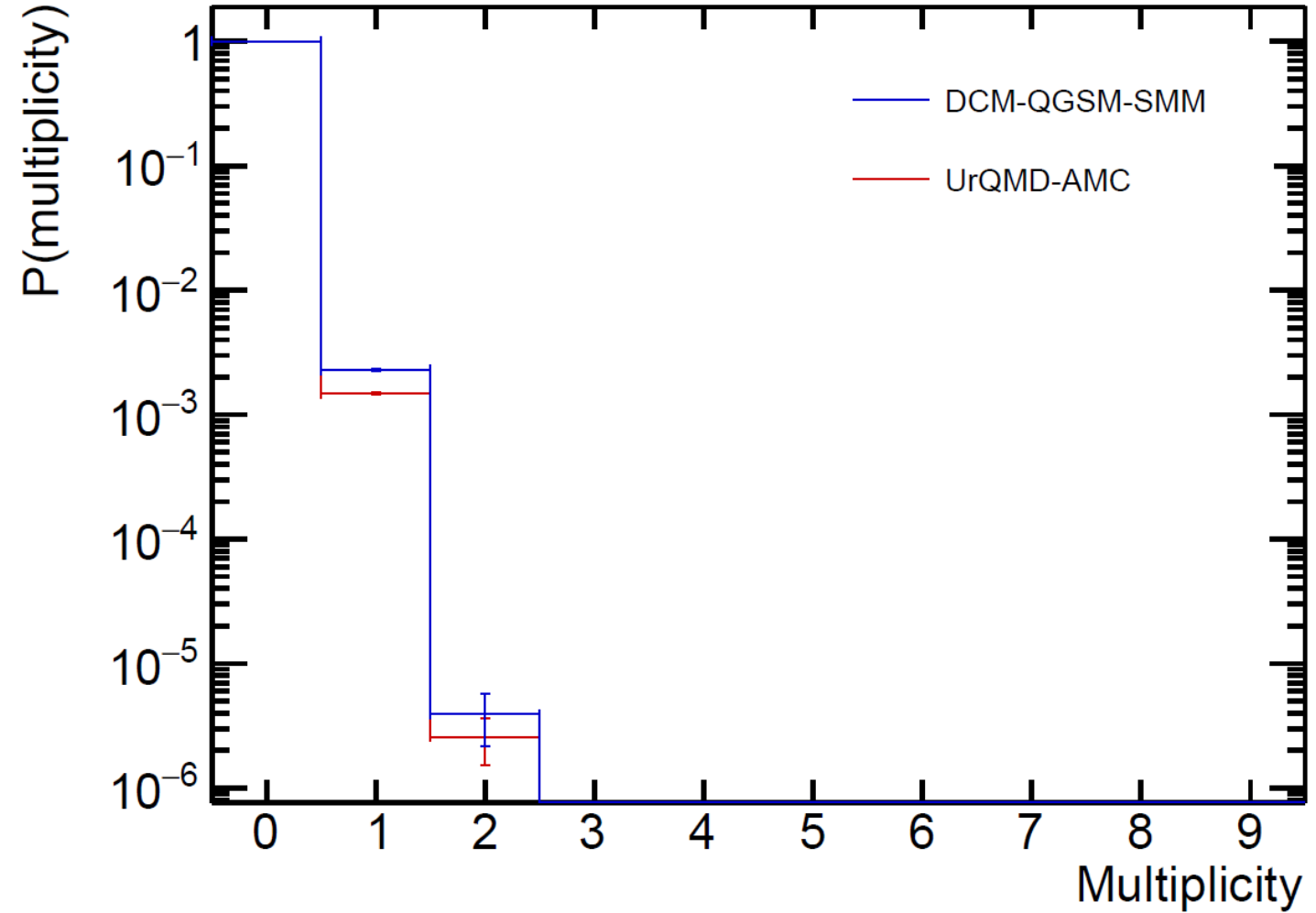
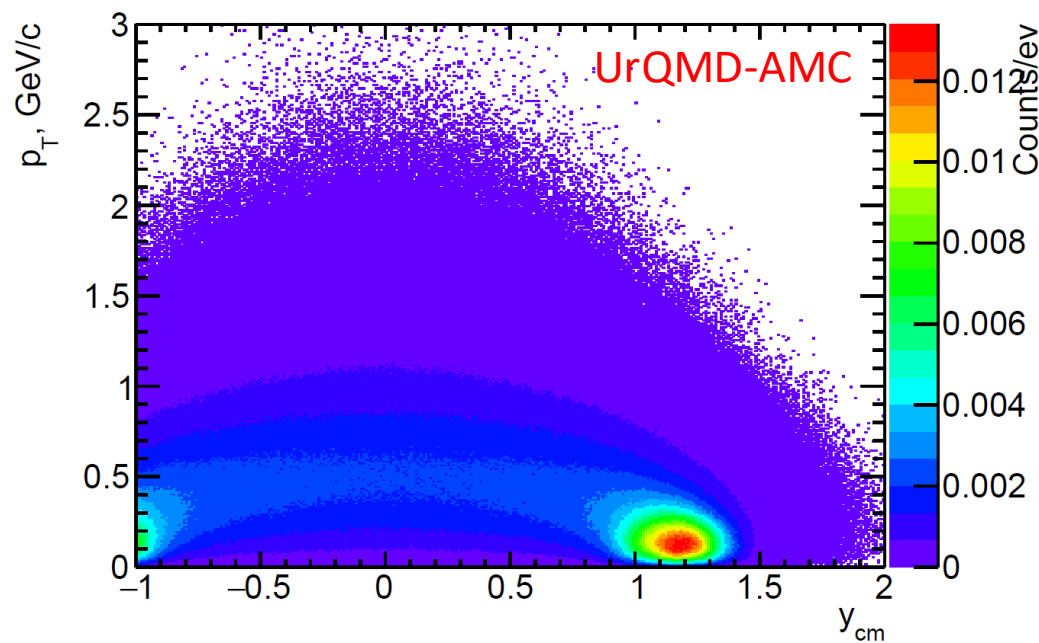
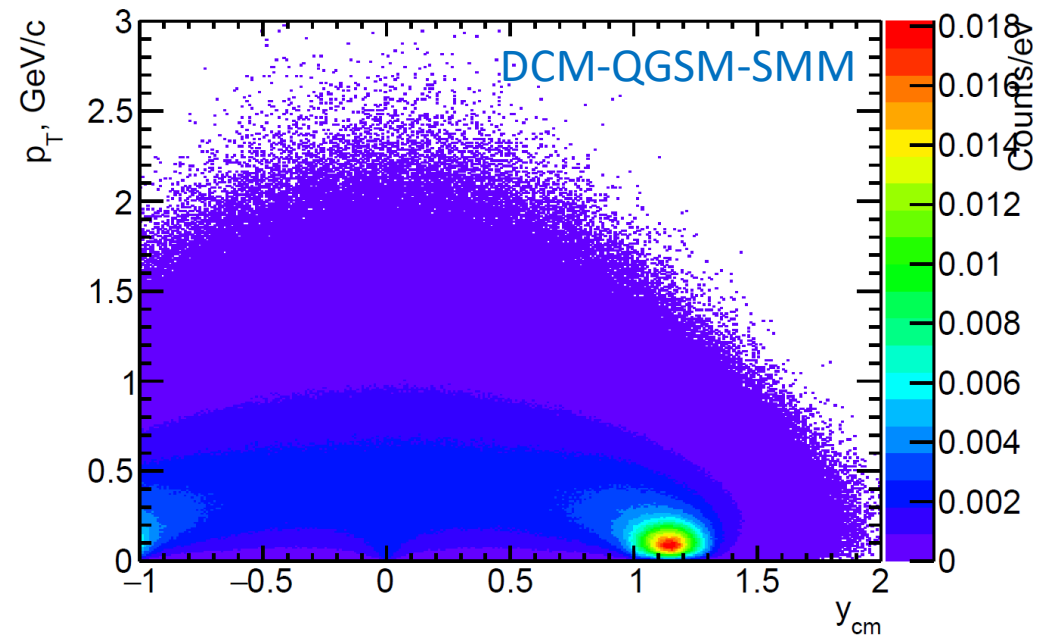
Nepeivoda, R. et al., Pre-Equilibrium Clustering in Production of Spectator Fragments in Collisions of Relativistic Nuclei. *Particles* **2022**, 5, 40–51.





27°

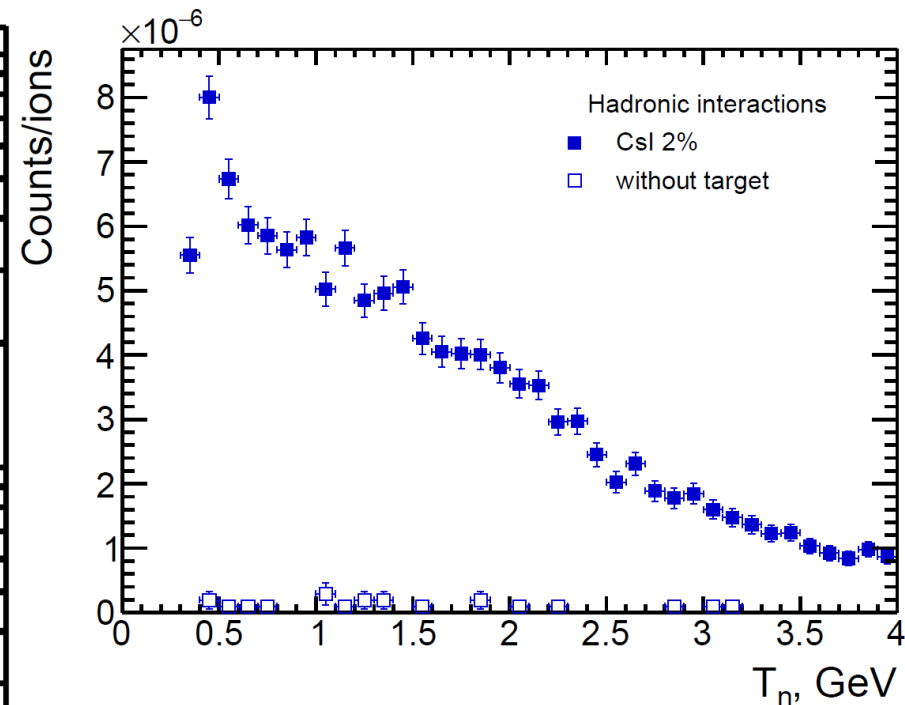
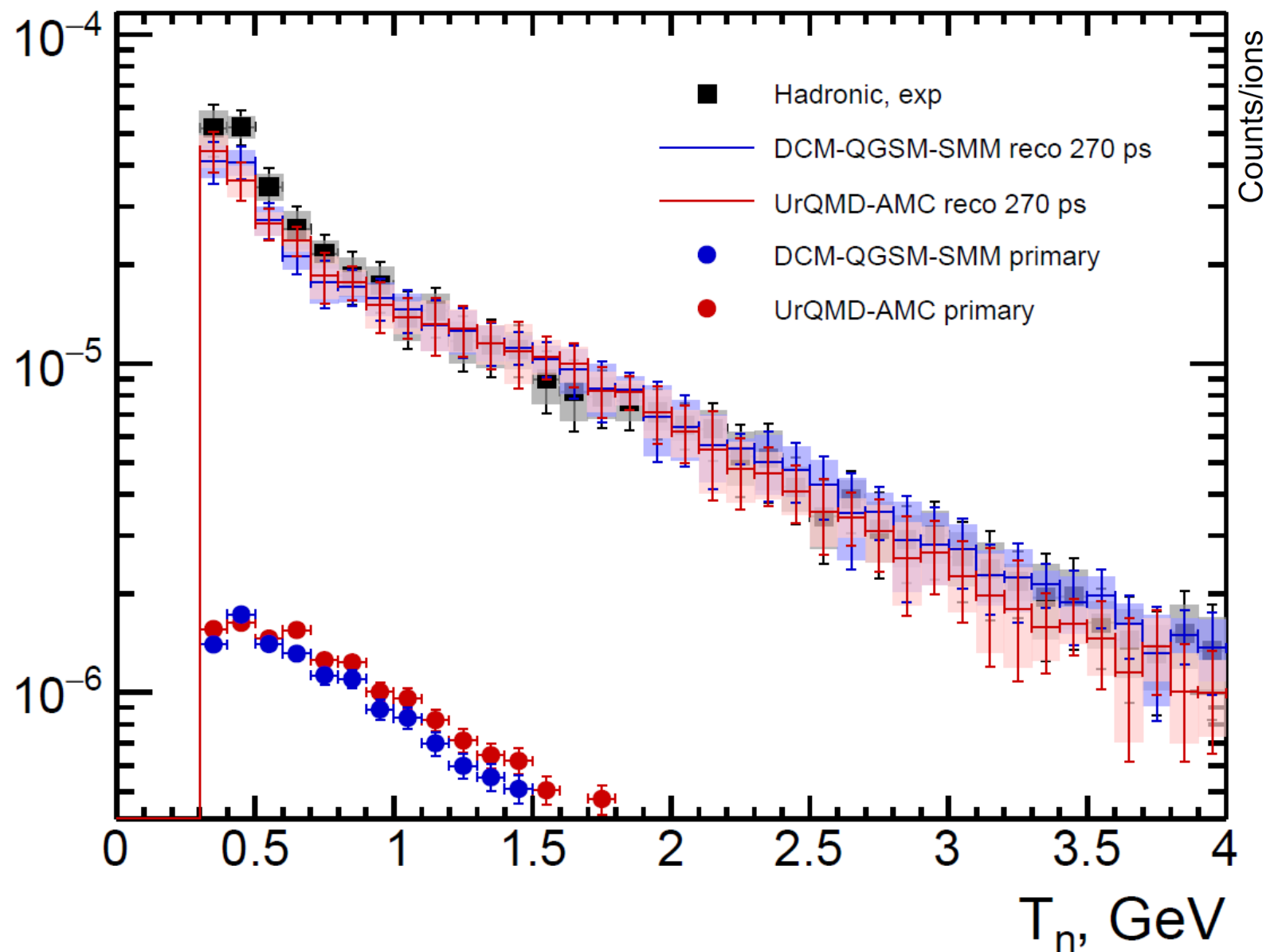
Neutron yields at 27°



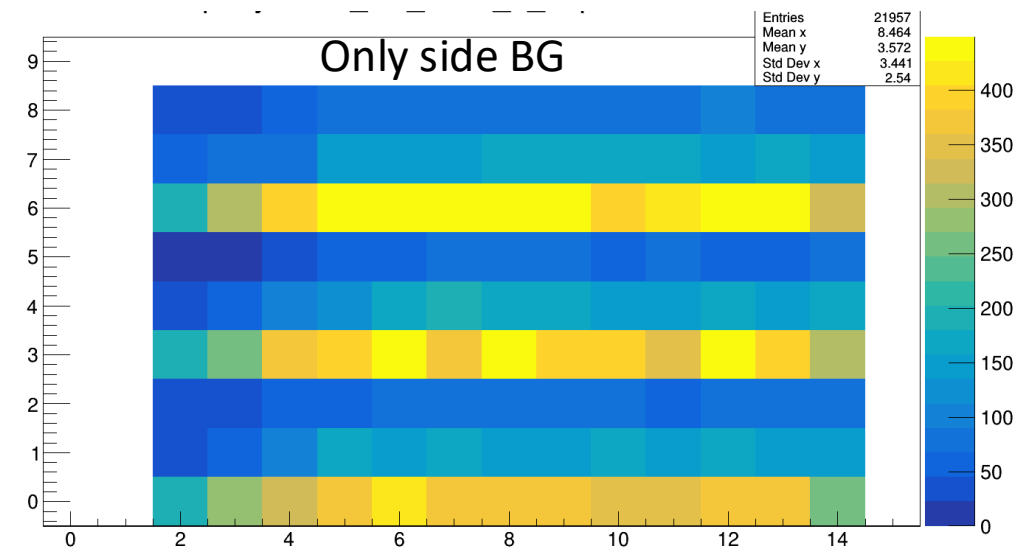
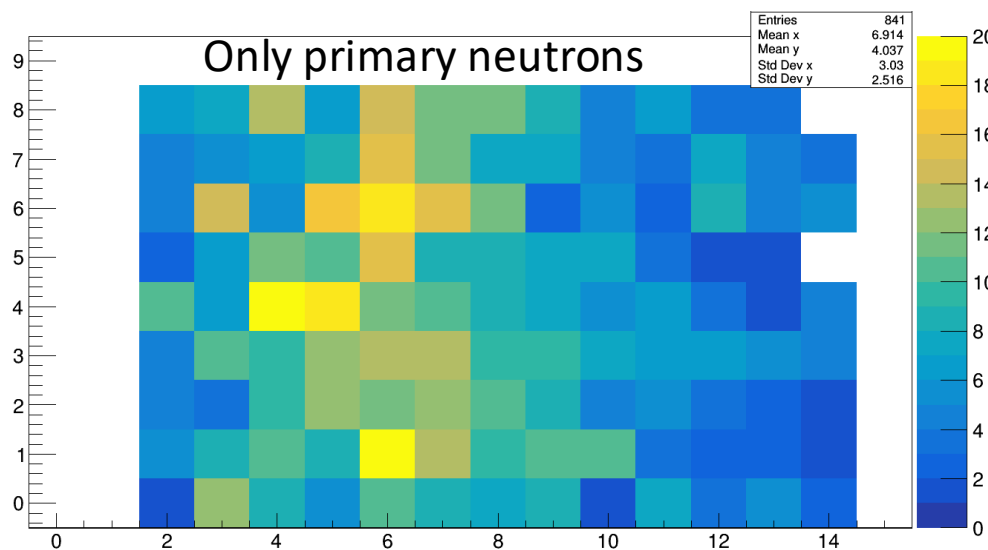
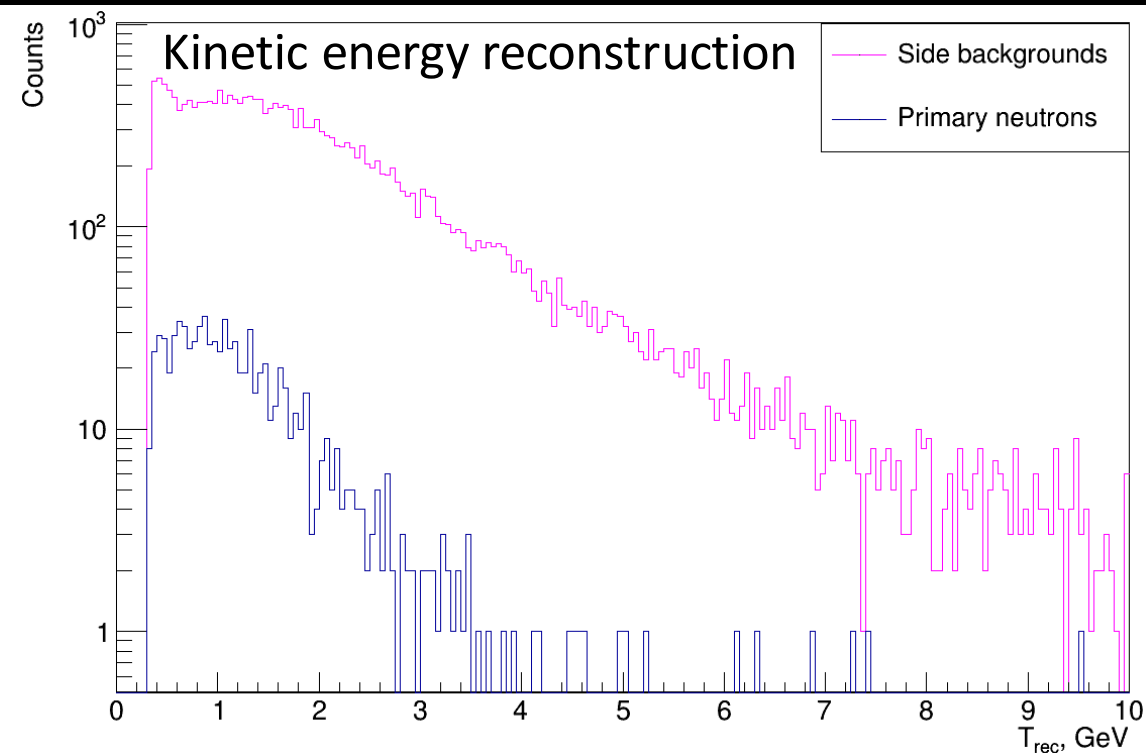
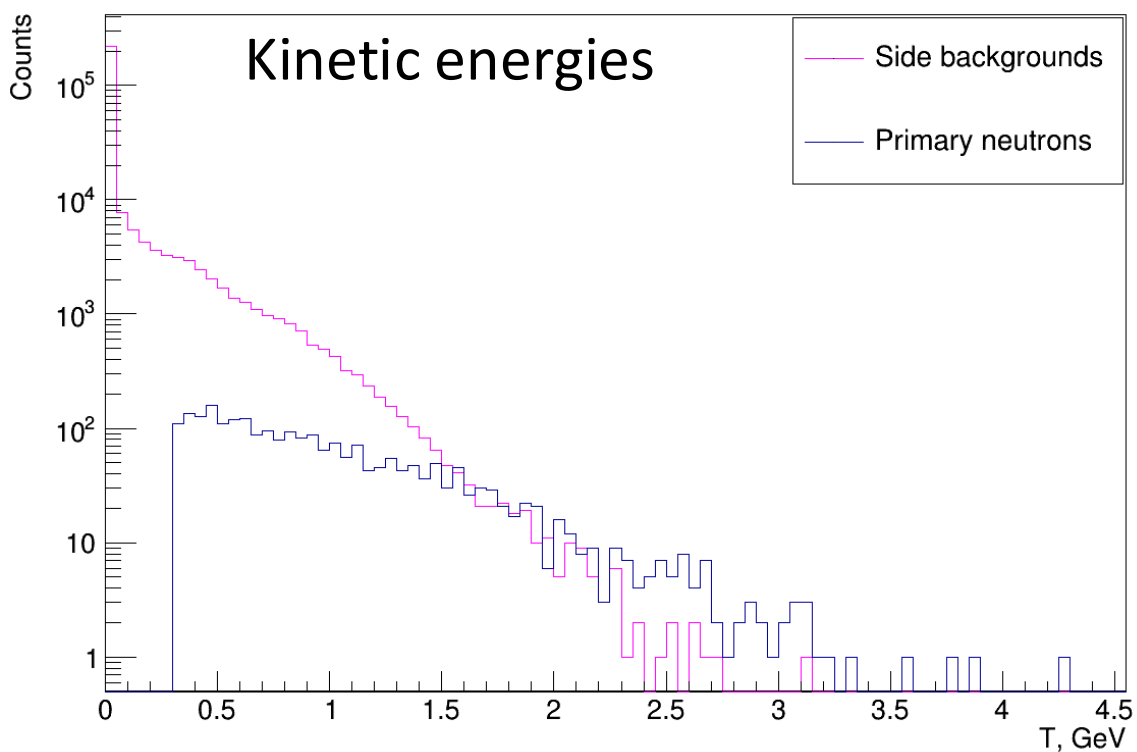
Neutron yields at 27°



Counts/ions



Backgrounds DCM-QGSM-SMM



Experimental data
Kinetic energy reconstruction

